Computational and experimental studies of reactive intermediates in glycosylation reactions

Remmerswaal, W.A.

Chapter 7

Anomeric Triflates versus Dioxanium Ions: Different Product-Forming Intermediates from 3-Acyl Benzylidene Mannosyl and Glucosyl Donors

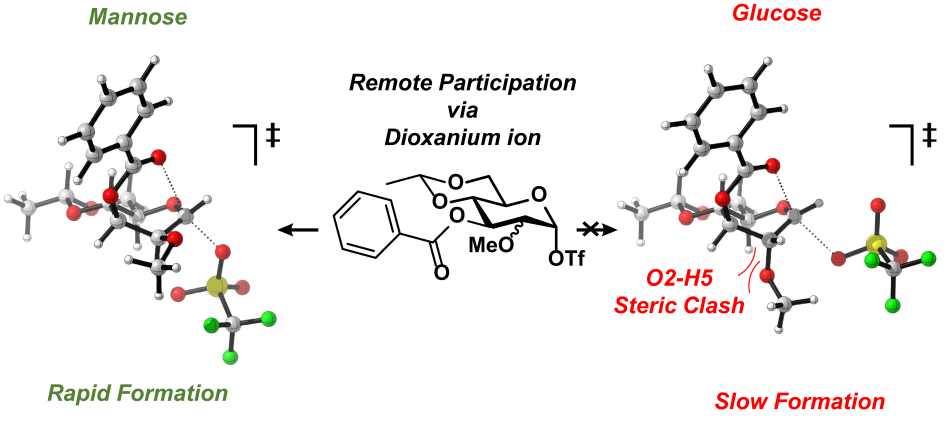

Abstract | Minimal structural differences in the structures of glycosyl donors can have a tremendous impact on their reactivity and the stereochemical outcomes of their glycosylation reactions. Here, a combination of systematic glycosylation reactions, the characterization of potential reactive intermediates, and in-depth computational studies is used to study the disparate behavior of glycosylation systems involving benzylidene glucosyl and mannosyl donors. While these systems have been studied extensively, no satisfactory explanations are available for the differences observed between the 3-*O*-benzyl/benzoyl mannose and glucose donor systems. The potential energy surfaces of the different reaction pathways available for these donors provide an explanation for the contrasting behavior of the seemingly similar systems. Evidence has been provided for the intermediacy of benzylidene mannosyl 1,3-dioxanium ions, while the formation of the analogous 1,3-glucosyl dioxanium ions is thwarted by a prohibitively strong flagpole interaction of the C-2-*O*-benzyl group with the C-5-proton in moving towards the transition state in which the glucose ring adopts a $B_{2,5}$-conformation. This study provides an explanation for the intermediacy of 1,3-dioxanium ions in the mannosyl system and an answer as to why these bridged cations do not form from analogous glucosyl donors.

Published | Remmerswaal, W. A.; Elferink, H.; Houthuijs, K. J.; Hansen, T.; ter Braak, F.; Berden, G.; van der Vorm, S.; Martens, J.; Oomens, J.; van der Marel, G. A.; Boltje, T. J.; Codée, J. D. C., *J. Org. Chem.* **2024**, *89* (3), 1618–1625.

Introduction

Controlling the stereochemistry in glycosylation reactions is crucial for the assembly of oligosaccharides and glycoconjugates, which are required as molecular tools in glycobiological, glycomedical, and glycomaterial studies. However, full control over the stereochemical outcome of glycosylation reactions continues to be a major challenge. The wide variety of structurally different glycans has spurred the development of many different strategies to steer the stereochemical outcome of a glycosylation reaction. Neighboring-group participation by acyl groups at C-2 is commonly used in the construction of 1,2-*trans* linkages. It is the most general means to control glycosylation stereoselectivity and it is relatively independent on the decoration pattern of the glycosyl donor.[1–3] For the construction of 1,2-*cis*-glycosyl linkages, no general strategy is available,[4–6] and translating methodology from one donor to another is often very challenging[7] if not impossible.

The Crich β-mannosylation methodology, in which a 4,6-*O*-benzylidene protecting group is used in conjunction with non-participating protecting groups at the C-2 and C-3 functionalities, has become one of the most powerful means to construct 1,2-*cis*-mannosyl linkages.[8,9] Strong evidence for the intermediacy of mannosyl α-triflates as product-forming intermediates in glycosylations following an S_N2-type mechanism has accumulated.[10] However, the method is sensitive to changes in the protecting group pattern, and when a C-3-acyl group is present, the donors give rise to highly stereoselective α-mannosylations reactions.[11–13] In contrast, benzylidene protected glucosyl donors provide mixtures of α/β-products, with the anomeric product ratio critically hinging on the nucleophilicity of the acceptor.[11,14,15] The stereoselectivity of these glucosylations appears to be relatively insensitive to changes in the protecting group at C-3,[16] although systematic studies have not been reported to dissect the influence of C-3 ester groups.

There has been significant debate as to the origin of the high α-selectivity in the 3-acyl benzylidene mannose case.[17–19] While Crich and co-workers initially postulated long-range participation as an explanation for this stereoselectivity,[20] they have more recently argued strongly against the possible formation of the 1,3-dioxanium ions because it requires the formation of a highly strained dioxanium ion from a C-3-acyl rotamer that is hardly populated, requiring an intramolecular substitution reaction on a high-energy ring conformer.[21–23] Rather, they argued that the C-3-ester destabilizes the anomeric triflate, promoting reactions through an oxocarbenium ion intermediate.[22,23] To investigate the formation of 1,3-mannosyl dioxanium ions, glycosylation reactions of 3-acyl-mannosyl donors were recently investigated with chemical exchange saturation transfer (CEST) NMR. Spectroscopic evidence was obtained for the generation of 1,3-dioxanium ions from 3-acyl-4,6-benzylidene mannosyl α-triflates, that can account for the formation of the observed α-products.[24–29] However, these CEST-NMR studies were not able to detect the corresponding glucosyl 1,3-dioxanium ions.

This report focusses on unraveling the origin of the contrasting behavior of the 3-acyl benzylidene mannosyl and glucosyl donors. Stereoselectivity trends were established through a combination of systematic glycosylation reactions, using a series of alcohol nucleophiles of gradually changing nucleophilicity. Gas-phase IR spectroscopy were used to study the potential formation of the 1,3-dioxanium ions, and computational experiments were used to investigate different reaction paths of the anomeric triflates. Combined with previous NMR studies[29] that have revealed the formation of mannosyl 1,3-dioxanium ions and the absence of these species from the corresponding glucosyl systems, a picture emerges on the diverging reaction pathways followed in the mannose and glucose systems. The computational studies pin-point the structural features responsible for the contrasting behavior of the mannosyl and glucosyl donors and illuminate the delicate balancing act between the various reactive intermediates. The study explains why long-range participation can take place in one donor (*i.e.,* the mannose system), but fails to control stereoselectivity in closely related systems (*i.e.,* the glucose donors).

Results and discussion

First, acceptor reactivity-stereoselectivity trends were established for the benzylidene mannosyl and glucosyl donors using a series of model acceptors of gradually increasing nucleophilicity (*i.e.*, 2,2,2-trifluoroethanol, TFE; 2,2-difluoroethanol, DFE; 2-fluoroethanol, MFE; ethanol, EtOH), in a set of pre-activation glycosylation reactions,[30,31] in which the glycosyl triflates are generated prior to the addition of the acceptors.[10] The results of these model glycosylation reactions are summarized in Table 1b. As previously reported,[11,14,15] the stereoselectivity of the glycosylation reactions of the 2,3-di-*O*-benzyl benzylidene glucose donor **1** gradually shifts from α- to β-stereoselectivity as the nucleophilicity of the acceptor increases. Conversely, the reactions of the 2,3-di-*O*-benzyl benzylidene mannose donor proceeded with β-selectivity irrespective of the reactivity of the nucleophile. Installation of a benzoate group on the C-3 of the glucosyl donor had no effect on the stereochemical outcome of the glycosylation reactions. However, a tremendous shift in stereoselectivity was observed for the glycosylations of the mannosyl donors, providing exclusively the α-product, in line with previous experiments with a 3-*O*-benzoyl-2,4,6-tri-*O*-benzyl mannosyl donor. Similar to the glycosylations of the corresponding 2,4,6-tri-*O*-benzyl donors, the stark contrast between the mannose and glucose series may be related to the formation of a dioxanium ion intermediate. As mentioned above, the mannosyl dioxanium ions could be detected in solution using CEST-NMR, while the glucosyl dioxanium ions were not observed.

Table 1. Model glycosylation reactions. The stereoselectivity of the reaction is expressed as α:β and based on ^{1}H-NMR of purified α/β-product mixtures. Blue-colored cells represent α-selectivity, while orange-colored cells represent β-selectivity. The percentage given between brackets represents the yield after purification by column chromatography. Pre-activation based glycosylation conditions: donor **1**-**4** (1 equiv), Tf_2O (1.3 equiv), Ph_2SO (1.3 equiv), TTBP (2.5 equiv), DCM (0.05 M), −80 to −60 °C, then add nucleophile (2 equiv) at −80 °C and allow to warm to −40 °C.

a)

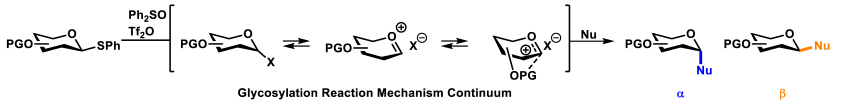

b)

	HOCF_3	HOCF_2H	HOCFH_2	HOCH_3
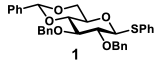 1	>98:2 (74%)	82:18 (95%)	50:50 (65%)	30:70 (80%)
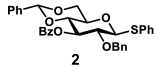 2	>98:2 (84%)	85:15 (74%)	45:55 (quant)	25:75 (quant)
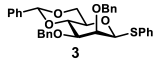 3	23:77 (51%)	18:82 (59%)	17:83 (61%)	19:81 (55%)
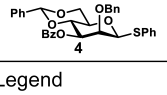 4	>98:2 (83%)	>98:2 (72%)	>98:2 (94%)	>98:2 (73%)

Legend

>90:10	>70:30	>50:50	<30:70	<10:90	(α:β)

To investigate this contrast between the mannosyl and glucosyl donors, the stability of the 1,3-dioxanium ions was investigated using ion IRIS[32] and computational chemistry (Figure 1a) because the relative stability of the dioxanium ions with respect to the parent oxocarbenium ions was found to correlate to the stereoselectivity of the acylated glycosyl donors.[26] To aid in spectroscopic elucidation, 2,3-di-*O*-methyl-4,6-ethylidene glucose (**5**) and mannose (**6**) donors were used. To obtain the cations of the sulfoxide donors, the proton adducts were generated by electrospray ionization (ESI+) and isolated in a Bruker AmaZon Speed ion trap (MS spectra can be found in Supplementary Figures S1 and S2).[33] Subsequently, the sulfoxide leaving group was expelled by collision induced dissociation (CID) to generate the glycosyl cations. An IR spectrum of the isolated cations was measured using the free-electron laser FELIX[34] in the 600-1900 cm^{-1} range by monitoring the wavelength-dependent IR multiple photon-induced dissociation (IRMPD) yield.[35]

The relative stabilities of the cations was assessed through a density functional theory (DFT) protocol in which the conformational energy landscape (CEL) maps for these cations were generated[26,36–38] This method maps the energy of the glycosyl cations as a function of their shape by probing the complete conformational space that these cations can occupy. The relative stabilities of the dioxanium ions *vs* the oxocarbenium ions for the glucosyl (Figure 1a) and the mannosyl (Figure 1b) cations were plotted. The CEL maps show that both the glucosyl and mannosyl 1,3-dioxanium ions are significantly more stable than their oxocarbenium ion counterparts, with a larger difference being found for the mannosyl ions (+9.2 kcal mol^{-1} *vs* +5.7 kcal mol^{-1}). Furthermore, the conformational space available to the glucosyl and the mannosyl cations is restricted. The 1,3-dioxanium ions preferentially take up (skew)boat-like conformations, *i.e.,* a $B_{2,5}$ and $^{1}S_{5}$ for the glucosyl and mannosyl dioxanium ions, respectively, in line with previous observations.[2,39] For the mannosyl cation, the CEL map diverges significantly from the CEL map of the 3-*O*-benzoyl-2,4,6-tri-*O*-benzyl-mannosyl 1,3-dioxanium cation, which adopts a $^{1}C_{4}$ conformation. In contrast, the conformation of the glucosyl 1,3-dioxanium cation ($B_{2,5}$) is relatively similar to that of its 4,6-di-benzylated counterpart. The restriction of conformational space is also apparent for the mannosyl oxocarbenium ion, which prefers to adopt a $B_{2,5}$ conformation. The conformational restriction, enforced by the benzylidene ring, thus prevents the benzylidene mannosyl 1,3-dioxolenium ion to adopt the electronically most favorable geometry (the $^{1}C_{4}$ conformation), rendering formation of the 3-*O*-benzoyl benzylidene mannosyl 1,3-dioxanium more difficult than the formation of its 4,6-di-benzyl counterpart, explaining the results previously obtained in CEST-NMR studies.[29,40]

The lowest energy conformers of the dioxanium and oxocarbenium cations were subsequently used to compute reference IR spectra to aid in interpretation of the experimentally obtained spectra.[26,41] Figure 1a/b show the computed spectra (filled) and the experimental spectra (black line) to confirm the formation of the dioxanium ions, as indicated by a characteristic dioxanium O-[C-O]$^{+}$ stretch (~1550 cm^{-1}) and the absence of the oxocarbenium [C1=O5]$^{+}$ (~1565 cm^{-1}), and benzoyl C=O (~1775 cm^{-1}) stretches. Overall, these results show that, in the gas-phase and in the absence of counterions, both the 3-acyl glucosyl and mannosyl donors can form bridged dioxanium ions. The fact that the dioxanium ions can form from both the glucosyl and mannosyl donors upon ionization in the gas-phase, but that only the mannosyl dioxanium ions form in solution, as judged from the CEST-NMR[22] and indirectly by the stereochemical outcome of the glycosylation reactions (Table 1), indicates that the pathways for the formation of these ions may diverge.

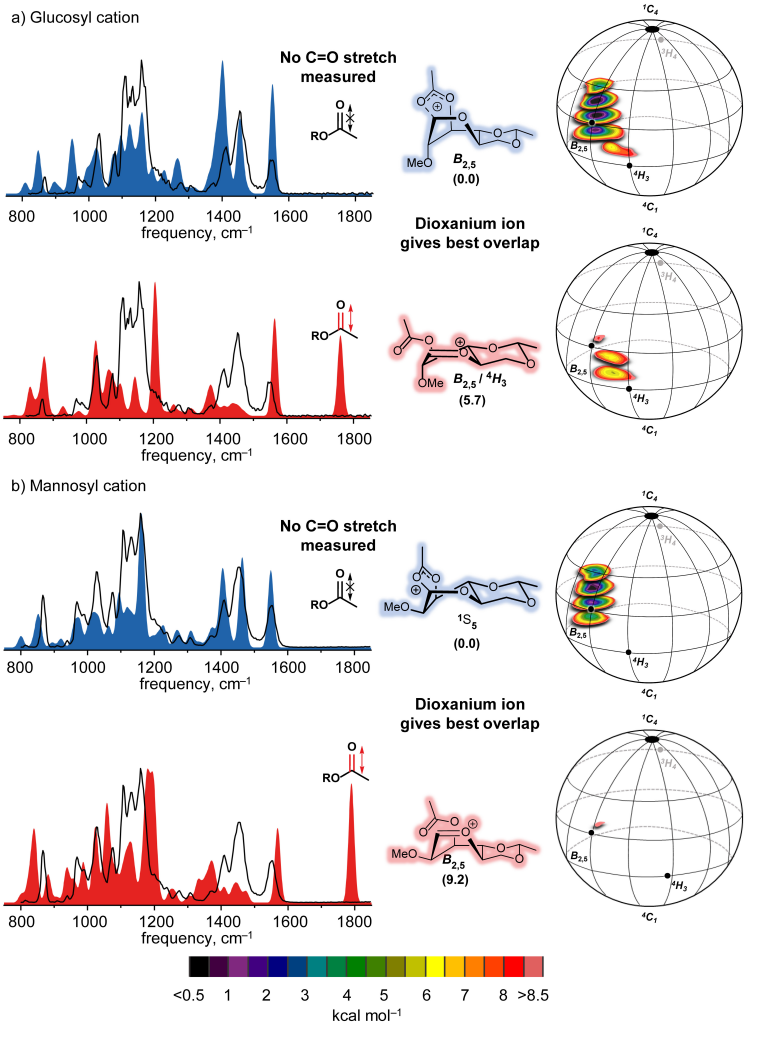

Figure 1. Conformational energy landscapes (CEL) and subsequent IR ion spectra (a) of 2-*O*-methyl-3-*O*-acetyl-4,6-*O*-ethylidene-glucosyl (b) and -mannosyl cation (c). For the CELs two acetyl ester rotamers (the oxocarbenium and dioxanium ion) were considered for all computed glycosyl cations generating two sperate CEL maps. All energies are as computed at B3LYP/6-311G(d,p) and expressed as gas-phase Gibbs free energy at 298.15 K in kcal mol^{-1}. The computed IR-spectra (filled) are compared with the measured IR-ion spectrum (black line) of the oxocarbenium or dioxanium ion.

Therefore, the pathways that lead to the formation of the dioxanium ions from the parent anomeric triflates were probed using DFT computations (See Supporting Information Table S2 for all data of the stationary points of the reaction profiles). Figure 2a shows the reaction profiles for the formation of the dioxanium ions from 1-α-*O*-triflyl-2-*O*-methyl-3-*O*-benzoyl-4,6-*O*-ethylidene-glucose and mannose, each normalized to the individual anomeric α-triflate intermediate. The formation of the dioxanium ion consists of three consecutive steps starting from the most stable conformation of the 1-α-*O*-triflyl-2-*O*-methyl-3-*O*-benzoyl-4,6-*O*-ethylidene-glycoside/mannoside (**R$_\alpha$**). The C-3 benzoate ester group first rotates around the H3-C3-O3-C$_{benzoyl}$ bond (**TS$_I$**), transitioning the H3-C$_{benzoyl}$ relation from a *syn* to an *anti*-orientation, to form an intermediate in which the benzoate ester is positioned above the ring (**RC$_I$**). This transformation proceeds with a significant energy barrier, as previously postulated by Crich,[22] and is somewhat more difficult for the mannoside (+9.6) than the glucoside (+8.3), as a result of torsion between the mannosyl benzoate ester and the axial C-2 group. The conformation of the ring then changes via **TS$_{II}$** to give a $B_{2,5}$ conformation (**RC$_{II}$**). The order of these two events was also changed (chair to boat transition before benzoate rotation), but this sequence provided higher energy pathways (see Supplementary Information Figure S3). Finally, the benzoate ester displaces the anomeric triflate (**TS$_{III}$,** Figure 2b and c) to form the triflate anion-stabilized dioxanium ion (**PC**). This step requires significantly more energy for the glucoside (+19.9) than for the mannoside (+11.4 kcal mol^{-1}). Notably, for the mannoside, the height of this transition state (**TS$_{III}$-man**) is similar to **TS$_{II}$**, indicating that expulsion of the triflate is rather favorable when the mannoside adopts the correct geometry. Repositioning of the triflate towards the carbonyl carbon of the benzoate group then forms the final triflate stabilized dioxanium ion (**P**), in which the α-face of the dioxanium ion is available for nucleophilic attack. Similar to the **PC** and the solvent separated dioxanium ion (Supplementary Table S2), the **P-man** (+9.9) is much more stable than the **P-glu** (+13.0).

Conversely, for the formation of the glucosyl dioxanium ion, expulsion of the anomeric triflate presents the highest overall barrier on the potential energy surface. To understand the differences in barrier height for **TS$_{III}$ man/glu**, the structures surrounding the transition states were examined: **RC$_{II}$**, **TS$_{III}$**, **PC** and **P**. From the computed reaction profiles, the relative Gibbs free energy **RC$_{II}$-glu** is slightly higher than of **RC$_{II}$-man**, while the energy of **PC-man** and **PC-glu** are different. Thus, the difference in energy between **TS$_{III}$-man** and **TS$_{III}$-glu** develops in going towards the transition state. When the conformations of **RC$_{II}$**, **TS$_{III}$**, **PC** and **P** are compared, it is noted that the conformations of the glucose and mannose stationary points are virtually identical (*i.e.*, $B_{2,5}$-like) in this part of the reaction profiles, and that during the transitioning between these points only minimal conformational changes occur.

As the energy difference does not originate from the gluco and manno stationary points having different ring conformations, the interactions of the ring substituents in the gluco and manno systems were compared. In the $B_{2,5}$ conformers, flagpole interactions of the axial C-2 and C-5 substituents are a major contributor of the ring strain. For the mannoside, this interaction is between two protons, while the in glucoside it is a more severe oxygen-hydrogen interaction. In going to **TS$_{III}$**, the C-2 and C-5 substituents are brought closer together (See Figure 2b,c) to forge the bond between C-1 and the benzoyl carbonyl group, increasing the flagpole interactions, leading to a significantly higher energy penalty for the glucoside than for the mannoside. In addition, the triflate leaving group in the mannoside can be positioned in a more favorable orientation, allowing interaction between the triflate and the H-2 and H-5 protons. For the glucoside, this orientation would lead to unfavorable electrostatic repulsion between the pseudo axial triflate and the C-2 oxygen substituent. Instead, the glucose triflate avoids this steric clash through a different orientation, in which there is less interaction with the *O*-2. As a result, the transition state for the glucose system is significantly later, with the triflate further away from the positive charge, leading to an increase in energy.[42]

Finally, the pathway for the formation of the anomeric β-triflate (**R_β**) from its α-anomer was probed. This *in situ* anomerization scheme has been forwarded to account for the formation of the α-glucosyl products, while it has been excluded for the mannosyl case because of the presumed instability of the β-mannosyl triflate. Indeed, Asensio and co-workers have previously been able to detect the β-glucosyl triflate by NMR spectroscopy of an ^{13}C-labeled glycosyl triflate.[43] The elusive β-mannosyl triflate was detected by $^{1}H/^{19}F$ CEST,[29] highlighting the need to revisit the anomerization reaction in both cases. As shown in the reaction profiles for the glucosyl and mannosyl triflates (Figure 2a, left pathways), the activation energy (**TS_{IV}**) for the formation of the anomeric β-triflate (**R_β**) is slightly higher for the mannoside (+16.5 kcal mol^{-1}) than for the glucoside (+15.8 kcal mol^{-1}). When the entire potential energy surface is regarded, the key distinction between the mannoside and the glucoside reaction profiles becomes apparent: for the glucosyl triflate, it is energetically more favorable to form the β-triflate (+15.8 kcal mol^{-1}) than the dioxanium ion from the α-triflate (+19.9 kcal mol^{-1}), while for the mannosyl triflate the reverse is true (**TS_{IV}** and **TS_{III}** are, respectively, +16.5 kcal mol^{-1} and +11.4 kcal mol^{-1}). The formation of the two different reactive intermediates accounts well for the dichotomy in the stereochemical outcome for the 3-*O*-benzoyl benzylidene mannose and glucose systems. The mannosyl dioxanium ion, detected by ^{13}C CEST NMR,[29,40,44] is responsible for the stereoselective formation of the α-mannosyl glycosylation products. In contrast, the glucosyl 1,3-dioxanium ion could be formed and characterized in the gas-phase, but no evidence was found in solution. In this case, the generation of the mixtures of anomeric products can be explained using the anomeric triflates as product-forming intermediates, with reactive nucleophiles being capable of displacing the more prevalent α-glucosyl triflate and the weaker nucleophiles reacting with the more reactive β-triflates. As the pathway towards the glucosyl 1,3-dioxanium ion requires significantly more energy than the formation of the reactive β-triflate, as revealed by the computed potential energy surfaces, these ions do not partake in the reaction. This fact explains the analogous behavior of the 3-*O*-benzyl and 3-*O*-benzoyl benzylidene glucosyl donors. As the glucosylation reactions with the 2,3-di-*O*-benzyl benzylidene donors proceeded with identical stereoselectivity, it is likely they proceed through a similar S_N2-like mechanism.[45,46]

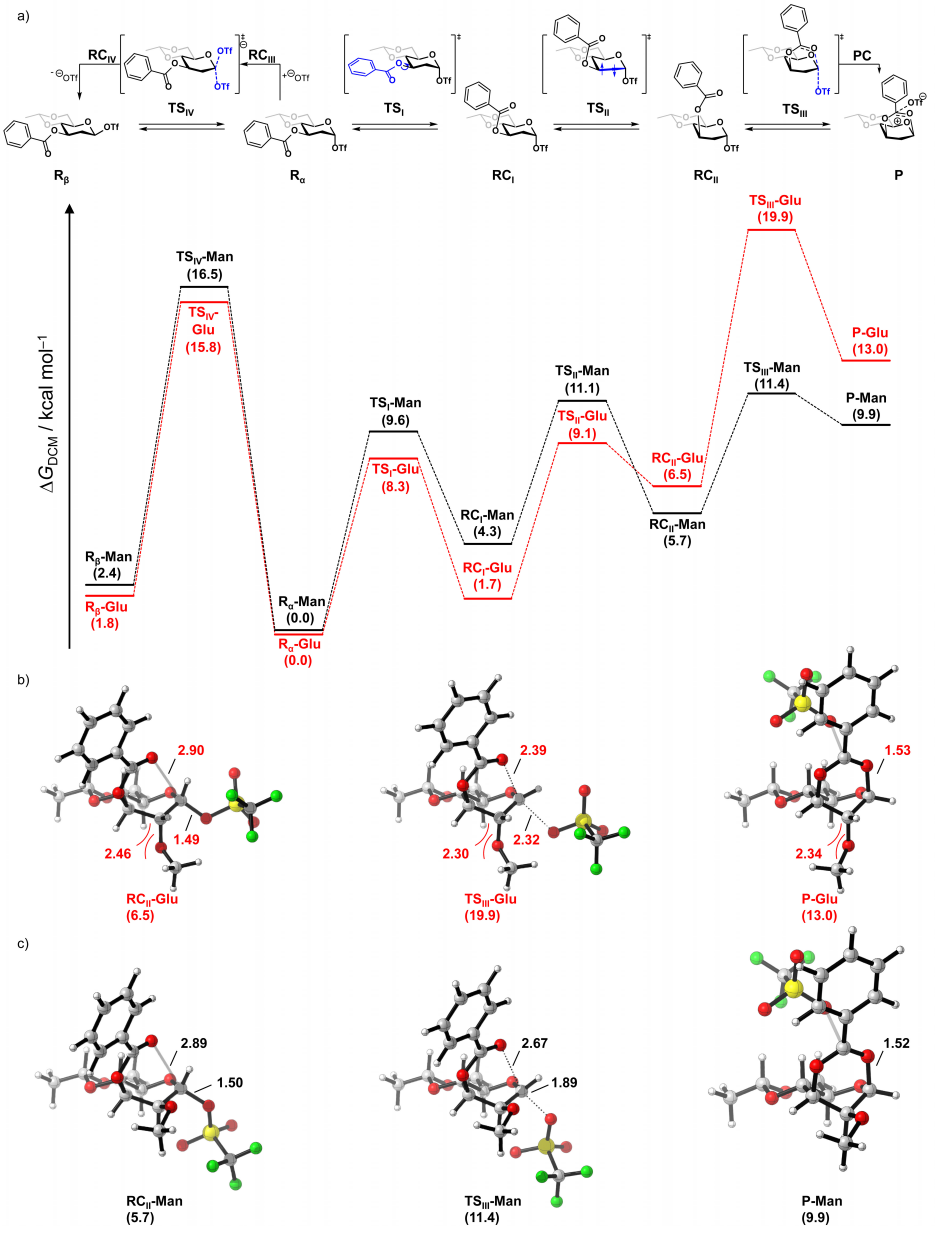

Figure 2. a) The computed reaction profiles for the formation of the dioxanium ion and anomeric β-triflate from α-1-*O*-triflyl-2-*O*-methyl-3-*O*-benzoyl-4,6-*O*-ethylidene glucose (**R_{α}-Glu**) and mannose (**R_{α}-Man**). For clarity the C-2 substituent is removed in all structures in Figure 2a. Gibbs free energies in dichloromethane (T = 213. 15K, ΔG_{DCM}, in kcal mol^{-1}) are given relative to the anomeric α-triflate **R_{α}** for each separate potential energy surface. Structures of **RC_{II}**, **TS_{III}**, **PC** and **P** for the (c) mannoside and (d) glucoside, were visualized by Cylview.[47] Distances are given in Å. Computed at PCM(CH_2Cl_2)–M06-2X/6-311++G(d,p)//PCM(CH_2Cl_2)–B3LYP-D3BJ/6-31+g(d). See Supporting Information Table S2 for all data of the stationary points of the reaction profiles.

Conclusions

In conclusion, the computational studies, combined with the series of systematic glycosylation reactions, and spectroscopic analysis of reactive intermediates have provided a detailed picture of the disparate glycosylation pathways of 2-*O*-benzyl-3-*O*-benzoyl-4,6-*O*-benzylidene mannosyl and glucosyl triflates. The study provides an explanation how minimal changes in donor structure (*i.e.,* the stereochemistry of a single stereocenter or changing a single remote benzyl group for a benzoate) impacts the formation of different reactive intermediates. While it has previously been argued that 1,3-dioxanium ions cannot form from benzylidene mannosyl donors, spectroscopic evidence, -both in the gas-phase and in solution, and computational chemistry have shown these species to be favorable intermediates formed upon activation of the mannosyl donors. These species explain the "black-and-white" difference in stereochemical outcome of the 3-*O*-benzoyl *vs* the 3-*O*-benzyl benzylidene mannose donors, with the former providing solely α-mannosyl product and the latter predominantly the β-isomers. Furthermore, the computational studies in the glucose series support the intermediacy of a product-forming β-glucosyl triflate. The reaction pathways, reactive intermediates and substituent effects defined in this study will help in the interpretation of future glycosylation results and the design of ever more effective stereoselective glycosylation chemistry to generate more and more complex oligosaccharides and glycoconjugates to fuel glycobiological, -medical, and structural studies.

Supporting information

Ion spectroscopy in a modified ion trap mass spectrometer

The experimental apparatus is based on a modified 3D quadrupole ion trap mass spectrometer (Bruker, AmaZon Speed ETD) that has been coupled to the beam line of the FELIX infrared free electron laser (IR-FEL).[33,34] Ammonium adducts of each compound ($[M+NH_4]^+$) were generated by positive electrospray ionization from solutions of 10^{-6} M in 50:50 acetonitrile:water containing 2% ammonium acetate and introduced at 2 μl min^{-1}. The mass-isolated ions of interest were collisionally activated for 40 ms with an amplitude parameter of 0.2-0.4V to generate the relevant oxonium products. These fragment ions were subsequently mass isolated in an additional MS/MS stage and finally irradiated by the tunable mid-infrared beam. The FEL was tuned to provide 10 μs optical pulses at 10 Hz having 30–60 mJ pulse energy over the entire tuning range (bandwidth ~0.4% of the centre frequency). The pulse energy used for measurements was appropriately attenuated to avoid saturation of the signal. When a sufficient number of photons is absorbed, unimolecular dissociation occurs and generates frequency-dependent fragment ion intensities in the mass spectrometer. Relating the precursor ion intensity to the total fragmentation intensity in the observed mass spectra, according to Equation S1, for each frequency position generates an infrared spectrum (3 cm^{-1} step size).[35] The yield is obtained from several averaged mass spectra and is linearly corrected for laser power. The IR frequency is calibrated using a grating spectrometer.

$$yield = \frac{-\ln(1 - \sum I\ (fragment\ ions))}{\sum I\ (parent + fragment\ ions)} \quad \text{(S1)}$$

Simulation of IR spectra

Vibrational spectra of the candidate geometries were generated using a previously reported workflow.[26,41] A SMILES code for the oxocarbenium and C-1,C-3 dioxanium ions served as input for the cheminformatics toolbox RDKit.[48] For each ion, 500 random conformations were generated using the distance geometry algorithm, which were minimized using the MMFF94 forcefield. The 40 most distinct geometries were selected based on the root-mean-squared distance between them. The geometries served as input for semi-empirical PM6 minimization and vibrational analysis with Gaussian16 Rev. C.01.[49] The resulting geometries were filtered for duplicates and subsequently minimized at the B3LYP/6-31++G(d,p) level, followed by vibrational analysis. The harmonic vibrational frequencies were scaled by 0.975 and broadened using a Gaussian function with a full-width at half-maximum of 25 cm^{-1}, as to match the experimental peak widths.

Glycosyl cation MS spectra

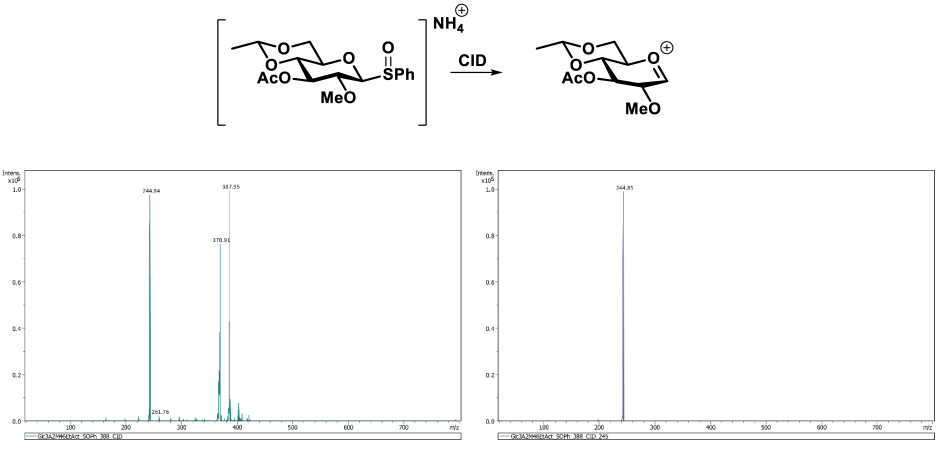

Supplementary Figure 1. MS spectra of the generation of the 3-*O*-acetyl-4,6-*O*-ethylidene-2-*O*-methyl-glucosyl cation by expelling the leaving group from the ammonium adduct using CID. Fragment with m/z 245 was isolated (right) following CID of the ammonium adduct parent ion (m/z 288) (left).

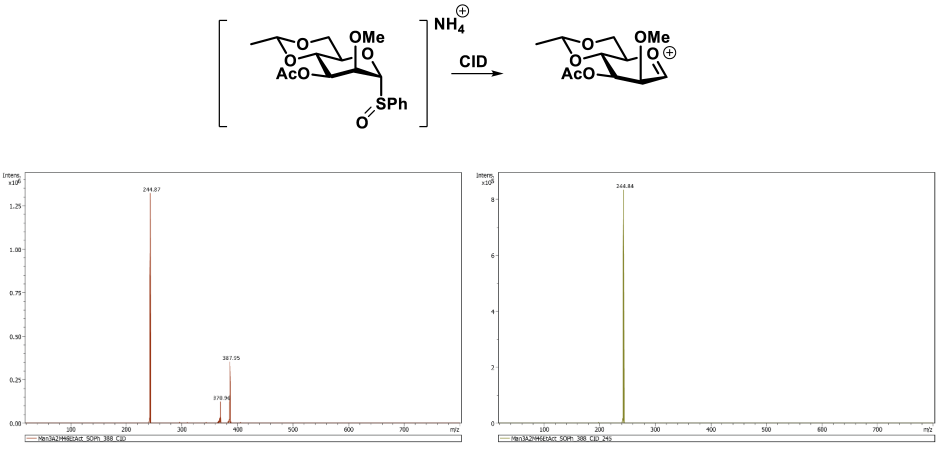

Supplementary Figure 2. MS spectra of the generation of the 3-*O*-acetyl-4,6-*O*-ethylidene-2-*O*-methyl-mannosyl cation by expelling the leaving group from the ammonium adduct using CID. Fragment with m/z 245 was isolated (right) following CID of the ammonium adduct parent ion (m/z 288) (left).

Supplementary Computational Methods

Computational methods: generation of potential energy surfaces

All computations were performed with Gaussian 09 Rev. D.01[50] at PCM(dichloromethane)-B3LYP-D3BJ-6-31+G(d) level of theory. Geometries were optimized without symmetry constraints. All calculated stationary points have been verified by performing a vibrational analysis, to be energy minima (no imaginary frequencies) or transition states (only one imaginary frequency). The character of the normal mode associated with the imaginary frequency of the transition state has been analyzed with an intrinsic reaction coordinate (IRC) calculation to ensure that it is associated with the reaction of interest.

Computational methods: generation of the computational energy landscapes

The initial structure for the conformational energy landscape (CEL) mapping of the six-membered glycosyl cation was optimized by starting from a 'conformer distribution search' option included in the Spartan 14[51] program by utilizing MM as the level of theory and MMFF[52] as the method. All generated geometries were re-optimized with Gaussian 09 Rev. D.01[50] by using B3LYP/6-311G(d,p), after which a vibrational analysis was computed to obtain the thermodynamic properties. The geometry with the lowest energy was selected as the starting point for the CEL. A complete survey of the possible conformational space was done by scanning three dihedral angles ranging from −60° to 60°, including the C1-C2-C3-C4 (D1), C3-C4-C5-O (D3) and C5-O-C1-C2 (D5). The resolution of this survey is determined by the step size which was set to 15° per puckering parameter, giving a total of 729 prefixed conformations per glycosyl cation spanning the entire conformational landscape. All other internal coordinates were unconstrained. Except when a C2-substituent was present on the oxocarbenium ring of interest, then the C2-H2 bond length was fixed based on the optimized structure to counteract rearrangements occurring for higher energy conformers. The 729 structures were optimized in the gas-phase with B3LYP/6-311G(d,p), after which a vibrational analysis was computed to obtain the thermodynamic properties. For this specific study two rotamers were taken into account, depending on the orientation of the C-2 acetyl protecting group (R1, C=O oriented towards C-1, in a way that makes C-1,C-3 dioxanium ion formation geometrically feasible. R2, C=O oriented away from C-1, in a way that makes C-1,C-3 dioxanium ion formation geometrically impossible.). For each rotamer CEL maps were separately computed and visualized. The $\Delta G^{T}_{gas,QH}$ were computed using the quasi-harmonic approximation in the gas-phase according to the work of Truhlar using the goodvibes suite.[54,55] The quasi-harmonic approximation is the same as the harmonic oscillator approximation except that vibrational frequencies lower than 100 cm^{-1} were raised to 100 cm^{-1} as a way to correct for the breakdown of the harmonic oscillator model for the free energies of low-frequency vibrational modes. All optimized structures were checked for the absence of imaginary frequencies. To visualize the energy levels of the conformers on the Cremer-Pople sphere, slices were generated dissecting the sphere that combine closely associated conformers. The OriginPro software was employed to produce the energy heat maps, contoured at 0.5 kcal/mol.[56] For ease of visualization, the Cremer-Pople globe is turned 180° with respect to its common representation.

Importance of the order of conformational change to form RC_{II}

In the main text only one order of conformational change to form **RC_{II}** is discussed: first the 2-*O*-benzoyl rotates, changing its orientation of the H3-$C_{Benzoyl}$ from syn to anti forming **RC_{I}**. Subsequently, **RC_{I}** undergoes a conformational change from the starting $^4C_1$ conformation towards the $B_{2,5}$ of **RC_{II}**. Although other pathways can be identified, this specific order of conformational change is energetically the most favorable. The main determinant of this pathway is the rotation of the benzoate. This rotation preferentially occurs from the starting chair conformation. Rotation from the $B_{2,5}$ conformation is rather unfavorable for both the manno- and glucoside, yielding $\Delta\Delta G_{4C1\text{-}B2,5}$ of respectively +4.9 and +3.1 kcal mol^{-1} (Supplementary Figure 3). This preference is due to a stronger interaction between the manno- and glucoside benzoate ester and the neighboring protons, as a result of the top side of the $B_{2,5}$ conformation being more crowded compared to the $^4C_1$ conformation.

Computing reaction profiles of various other 3-*O*-acyloxy-donors.
In previous research employing ^{1}H-CEST-NMR, observing the 3-*O*-benzoyl-2-*O*-benzyl-4,6-*O*-benzylidene mannose dioxanium ions has been difficult,[29] even though these donors (Table 1) show remarkable stereoselectivity. This inability to observe the 3-*O*-benzoyl-2-*O*-benzyl-4,6-*O*-benzylidene mannose dioxanium ions is not completely surprising, since ^{1}H-CEST-NMR has a quite narrow range for observable reaction rates. Replacing either the 3-*O*-benzoyl group with a 3-O-*p*-OMe-benzoyl (p-anisoyl) or the 4,6-*O*-benzylidene group with 4,6-di-*O*-methyl groups, lead to observable dioxanium ions. To corroborate these results, the above-mentioned reaction profiles for the formation of the dioxanium ions from 1-α-*O*-triflyl-2,4,6-tri-*O*-methyl-3-*O*-benzoyl, 1-α-*O*-triflyl-2-*O*-methyl-3-*p*-*O*-benzoyl-4,6-*O*-ethylidene mannose (Supplementary figure 5 and 6) were computed. Variation of the protecting groups on C-3, C-4, and C-6 did not change the barrier heights for the formation of the dioxanium ion significantly. However, substitution of either the 3-*O*-benzoyl group with a 3-O-*p*-OMe-benzoyl (*p*-anisoyl) or the 4,6-*O*-benzylidene group with 4,6-di-*O*-methyl groups, lead to significant stabilization of the dioxanium ion **P** (Supplementary Table 1). These results match well with the observed ^{1}H-CEST-NMR results.

Supplementary Table S1. Relative stability of the solvent separated dioxanium ions (P), and formation of the dioxanium ion through TS_{III} compared to each corresponding anomeric α-triflate. Gibbs free energies in dichloromethane (ΔG_{DCM}, in kcal mol^{-1}) are given relative to the anomeric α-triflate R_α. Computed at PCM(CH_2Cl_2)–M06-2X/6-311++G(d,p)//PCM(CH_2Cl_2)–B3LYP-D3BJ/6-31+g(d).

Dioxanium ion (P)	**Relative dioxanium formation (TS_{III}) (ΔG_{DCM}, in kcal mol^{-1})**	**Relative dioxanium stability (P) (ΔG_{DCM}, in kcal mol^{-1})**
2-*O*-methyl-3-O-benzoyl-4,6-*O*-ethylidene mannosyl	11.4	10.8
2-*O*-methyl-3-*O*-*p*-OMe-benzoyl-4,6-*O*-ethylidene mannosyl	11.2	8.1
2,4,6-tri-*O*-methyl-3-*O*-benzoyl mannosyl	9.7	8.8

Supplementary reaction profiles

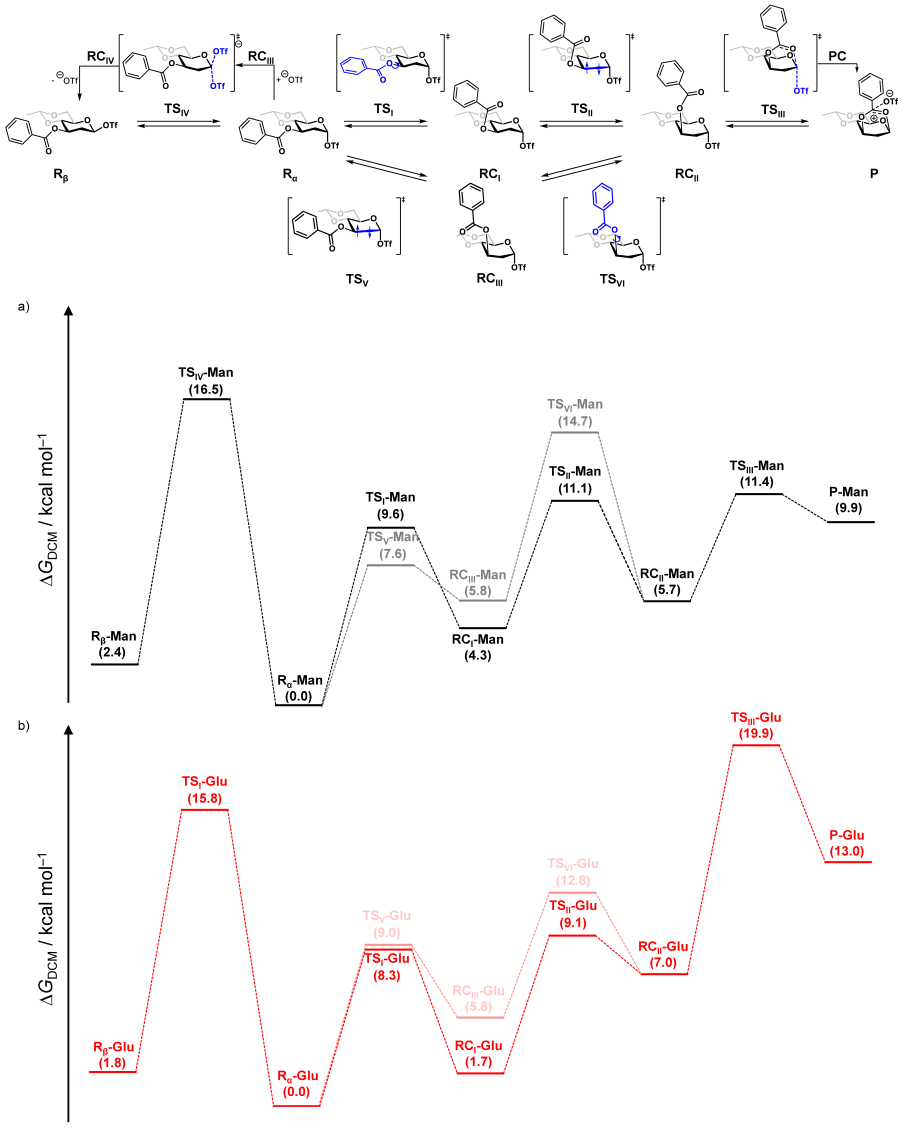

Supplementary Figure 3. The computed reaction profiles for the formation of the dioxanium ion and anomeric β-triflate from: a) α-1-*O*-triflyl-2-*O*-methyl-3-*O*-benzoyl-4,6-*O*-ethylidene glucose (R_α-Glu) and b) mannose (R_α-Man). For clarity the C-2 substituent is removed in all chemdrawings. Gibbs free energies in dichloromethane (ΔG_{DCM}, in kcal mol^{-1}) are given relative to the anomeric α-triflate R_α for each separate potential energy surface. Computed at PCM(CH_2Cl_2)–M06-2X/6-311++G(d,p)//PCM(CH_2Cl_2)–B3LYP-D3BJ/6-31+G(d). See Supporting Information Table S2 for all data of the stationary points of the reaction profiles.

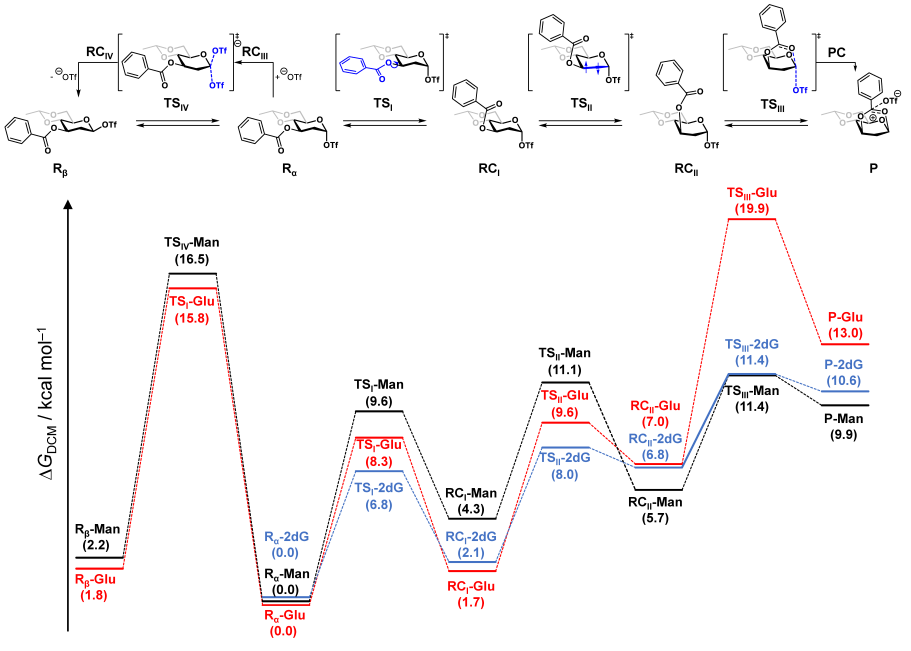

Supplementary Figure 4. The computed reaction profiles for the formation of the dioxanium ion and anomeric β-triflate from α-1-*O*-triflyl-2-*O*-methyl-3-*O*-benzoyl-4,6-*O*-ethylidene-glucose (R_α-Glu), α-1-*O*-triflate-2-deoxy-3-*O*-benzoyl-4,6-*O*-ethylidene-glucose (R_α-2dG) and α-1-*O*-triflyl-2-*O*-methyl-3-*O*-benzoyl-4,6-*O*-ethylidene-mannose (R_α-Man). For clarity the C-2 substituent is removed in all chemdrawings. Gibbs free energies in dichloromethane (ΔG_{DCM}, in kcal mol^{-1}) are given relative to the anomeric α-triflate R_α for each separate potential energy surface. Computed at PCM(CH2Cl2)–M06-2X//6-311++G(d,p)//PCM(CH2Cl2)–B3LYP-D3BJ/6-31+G(d). See Supporting Information Table S2 for all data of the stationary points of the reaction profiles.

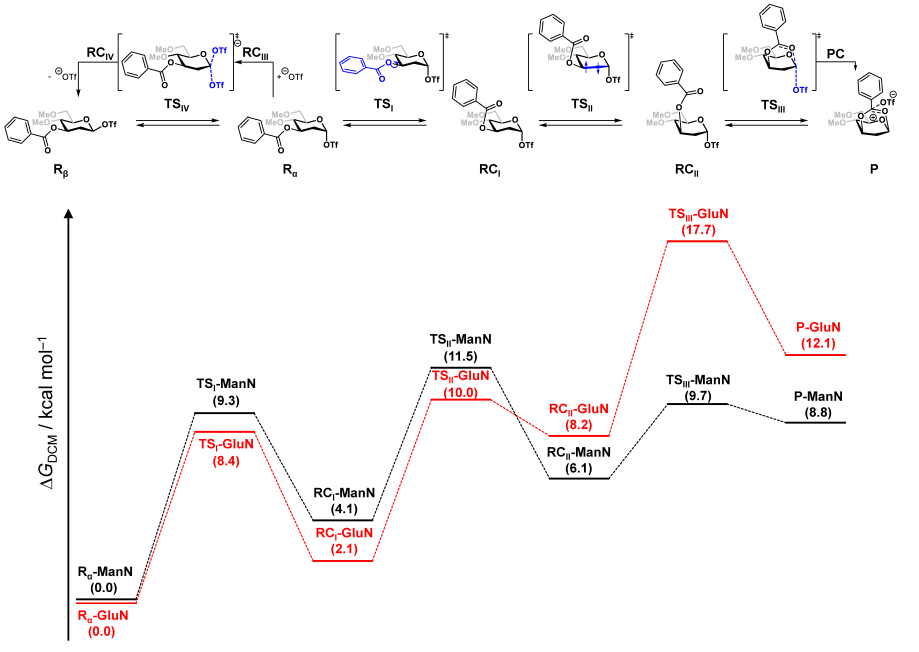

Supplementary Figure 5. The computed reaction profiles for the formation of the dioxanium ion and anomeric β-triflate from α-1-O-triflyl-2,4,6-tri-*O*-methyl-3-*O*-benzoyl-glucose (R_α-GluN), and mannose (R_α-ManN). For clarity the C-2 substituent is removed in all chemdrawings. Gibbs free energies in dichloromethane (ΔG_{DCM}, in kcal mol−1) are given relative to the anomeric α-triflate R_α for each separate potential energy surface. Computed at PCM(CH_2Cl_2)–M06-2X//6-311++G(d,p)//PCM(CH_2Cl_2)–B3LYP-D3BJ/6-31+g(d). See Supporting Information Table S2 for all data of the stationary points of the reaction profiles.

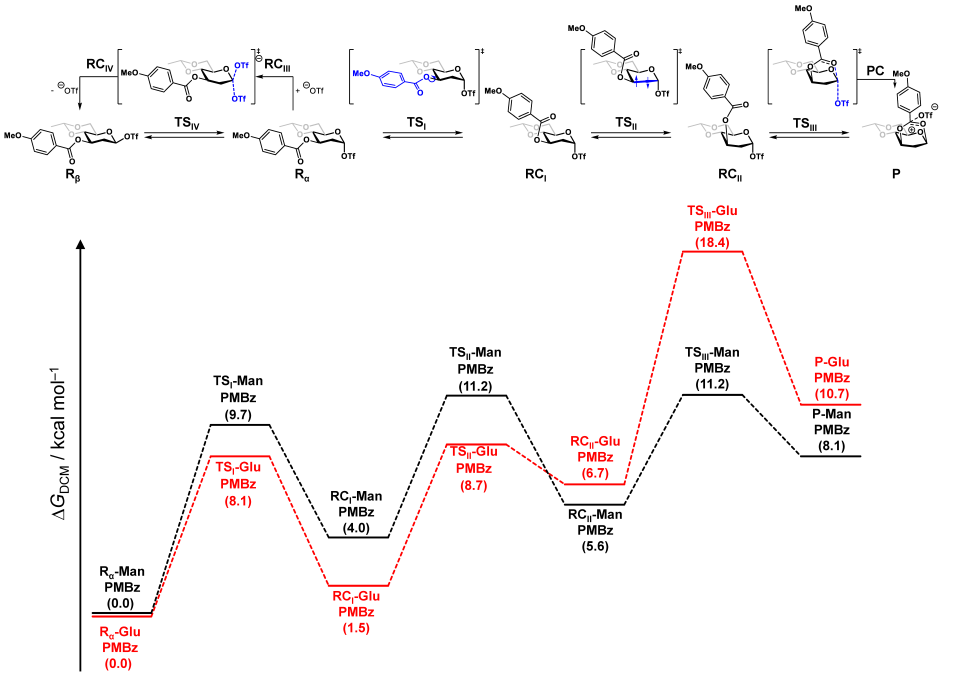

Supplementary Figure 6. The computed reaction profiles for the formation of the dioxanium ion and anomeric β-triflate α-1-*O*-triflyl-2-*O*-methyl-3-*O*-(4-*O*-methyl-benzoyl)-4,6-*O*-ethylidene-glucose (R_α-Glu) and mannose (R_α-Man). For clarity the C-2 substituent is removed in all chemdrawings. Gibbs free energies in dichloromethane (ΔG_{DCM}, in kcal mol^{-1}) are given relative to the anomeric α-triflate R_α for each separate potential energy surface. Computed at Computed at PCM(CH_2Cl_2)–M06-2X//PCM(CH_2Cl_2)–B3LYP-D3BJ/6-31+G(d). See Supporting Information Table S2 for all data of the stationary points of the reaction profiles.

Supplementary Organic Synthesis Methods

General experimental procedures

All chemicals (Acros, Fluka, Merck, and Sigma-Aldrich) were used as received unless stated otherwise. Dichloromethane was stored over activated 4 Å molecular sieves (beads, 8-12 mesh, Sigma-Aldrich). Before use traces of water present in the donor, diphenyl sulfoxide (Ph_2SO) and tri-*tert*-butylpyrimidine (TTBP) were removed by co-evaporation with dry toluene. The acceptors were stored in stock solutions (DCM, 0.5 M) over activated 3 Å molecular sieves (rods, size 1/16 in., Sigma-Aldrich). Trifluoromethanesulfonic anhydride (Tf_2O) was distilled over P_2O_5 and stored at –20 °C under a nitrogen atmosphere. Overnight temperature control was achieved by an FT902 Immersion Cooler (Julabo). Column chromatography was performed on silica gel 60 Å (0.04 – 0.063 mm, Screening Devices B.V.). TLC-analysis was conducted on TLC Silica gel 60 (Kieselgel 60 F254, Merck) with UV detection by (254 nm) and by spraying with 20% sulfuric acid in ethanol followed by charring at ± 150 °C or by spraying with a solution of $(NH_4)_6Mo_7O_{24}{\cdot}H_2O$ (25 g/l) and $(NH_4)_4Ce(SO_4)_4{\cdot}2H_2O$ (10 g/l) in 10% sulfuric acid in water followed by charring at ± 250 °C. High-resolution mass spectra were recorded on a Thermo Finnigan LTQ Orbitrap mass spectrometer equipped with an electrospray ion source in positive mode (source voltage 3.5 kV, sheath gas flow 10, capillary temperature 275 °C) with resolution R=60.000 at m/z=400 (mass range = 150-4000). ^{1}H and ^{13}C{^{1}H} NMR spectra were recorded on a Bruker AV-400 NMR instrument (400 and 101 MHz respectively), a Bruker AV-500 NMR instrument (500 and 126 MHz respectively), or a Bruker AV-850 NMR instrument (850 and 214 MHz respectively). For samples measured in $CDCl_3$ chemical shifts (δ) are given in ppm relative to tetramethylsilane as an internal standard or the residual signal of the deuterated solvent. Coupling constants (*J*) are given in Hz. To get better resolution of signals with small coupling constants or overlapping signals a gaussian window function (LB ± -1 and GB ± 0.5) was used on the ^{1}H NMR spectrum. All given ^{13}C APT spectra are proton decoupled. NMR peak assignment was made using COSY, HSQC. If necessary additional, HMBC and HMBC-GATED experiments were used to elucidate the structure further. The anomeric product ratios were based on the integration of ^{1}H NMR.

Preparation of the donors 1-4

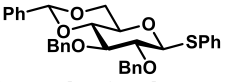

Phenyl 2,3-di-*O*-benzyl-4,6-*O*-benzylidene-1-thio-β-D-glucopyranoside (1). The title compound was prepared according to literature procedure.[11]

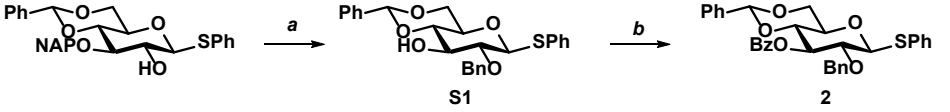

Supplementary scheme S1. Glucoside donor 2 synthesis. *Reagents and conditions:* a) 1. BnBr, NaH, DMF, 0 °C to RT; glucopyranoside; 2. DDQ, DCM:H_2O, **S1**: 82%; b) benzoyl chloride, pyridine, RT, **2**: quant.

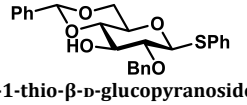

Phenyl 2-*O*-benzyl-4,6-*O*-benzylidene-1-thio-β-D-glucopyranoside (S1). The synthesis of **S1** started from phenyl 3-*O*-(2-naphthyl)methyl-4,6-*O*-benzylidene-1-thio-β-D-glucopyranoside[24] (1.34 g, 2.67 mmol), which was dissolved in dry DMF (10 ml, 0.25M) and cooled to 0 °C. Under inert atmosphere, NaH (60 Wt % dispersion in mineral oil, 0.16 g, 4.01 mmol, 1.5 equiv) was added portion wise and the reaction mixture was stirred for 10 minutes. Benzyl bromide (0.40 ml, 3.34 mmol, 1.25 equiv) was added and the reaction was stirred for 4 h while allowing to warm up to RT. Subsequently, the reaction was cooled to 0 °C and quenched with H_2O. The reaction mixture was diluted with H_2O and extracted with DCM. The organic layers were combined, washed with brine, dried over $MgSO_4$ and concentrated *in vacuo*. The crude reaction mixture was dissolved in DCM:H_2O (9:1, v:v, 15 ml, 0.2M), after which 2,3-Dichloro-5,6-dicyano-1,4-benzoquinone (0.910 g, 4,01 mmol, 1.5 equiv) was added. The reaction was protected from light and stirred for 1.5 h. The reaction was quenched by addition of sat. aq. $Na_2S_3O_3$ and filtered. The bi-phasic mixture was extracted with DCM. The organic layers were combined and washed with sat. aq. $NaHCO_3$, dried over $MgSO_4$, filtered and concentrated *in vacuo*. Flash column chromatography (100:0 → 80:20, pentane:EtOAc v:v) yielded the title compound (0.99 g, 2.19 mmol, 82%) as a white solid. TLC: R_f 0.18, (90:10, pentane:EtOAc, v:v); ^{1}H NMR (300 MHz, $CDCl_3$, HH-COSY, HSQC) δ 7.58 – 7.25 (m, 15H, CH_{arom}), 5.51 (s, 1H, C*H*Ph), 4.93 (d, J = 10.9 Hz, 1H, CH*H* Bn), 4.85 – 4.63 (m, 2Hz, H-1, C*H*H Bn), 4.35 (dd, J = 10.5, 4.8 Hz, 1H, H-6), 3.89 (td, J = 8.7, 2.5 Hz, 1H, H-3), 3.76 (dd, J = 10.5, 9.6 Hz, 1H, H-6), 3.58 – 3.33 (m, 3H, H-2, H-4, H-5), 2.58 (d, J = 2.5 Hz, 1H, 3-OH).; ^{13}C{^{1}H} NMR (75 MHz, $CDCl_3$, HSQC) δ 138.1 ($C_{q\text{-}arom}$), 137.0, 133.2, 132.3, 129.4, 129.2, 128.7, 128.5, 128.4, 128.2, 128.0, 126.4 (CH_{arom}), 101.9 (CHPh), 88.1 (C-1), 80.8 (C-2), 80.4 (C-4), 75.6 (CH_2 Bn), 75.5 (C-3), 70.2 (C-5), 68.7 (C-6); HRMS (ESI): $[M+Na]^+$ calcd for $C_{26}H_{26}O_5SNa$ 473.1393, found 473.1391.

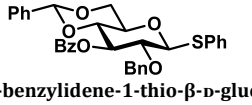

Phenyl 3-*O*-benzoyl-2-*O*-benzyl-4,6-*O*-benzylidene-1-thio-β-D-glucopyranoside (2). S1 (0.952 g, 2.11 mmol) was dissolved in pyridine (4 ml, 0.5 M), benzoyl chloride (0.445 g, 0.368 ml, 3.17 mmol, 1.5 equiv) was added and the reaction was stirred for 4 hours. It was diluted with ethyl acetate and sequentially washed with 1M HCl (aq.) and sat. aq. $NaHCO_3$. The organic layers were combined, dried over $MgSO_4$, filtered and concentrated *in vacuo*. Flash column chromatography (100:0 → 95:5, pentane:EtOAc v:v) yielded the title compound (1.26 g, quant) as a white solid. TLC: R_f 0.35, (90:10, pentane:EtOAc, v:v); ^{1}H NMR (400 MHz, $CDCl_3$, HH-COSY, HSQC, HMBC) δ 8.06 – 7.64 – 7.11 (m, 20H, CH_{arom}), 5.68 (dd, J = 9.8, 8.7 Hz, 1H, H-3), 5.49 (s, 1H C*H*Ph), 4.90 (d, J = 9.7 Hz, 1H, H-1), 4.85 (d, J = 10.5 Hz, 1H, CH*H* Bn), 4.61 (d, J = 10.5 Hz, 1H, C*H*H Bn), 4.40 (dd, J = 10.5, 4.9 Hz, 1H, H-6), 3.87 – 3.67 (m, 3H, H-2, H-4, H-6), 3.62 (td, J = 9.7, 5.0 Hz, 1H, H-5); ^{13}C{^{1}H} NMR (101 MHz, $CDCl_3$, HSQC, HMBC) δ 165.5 ($C_{q\text{-}benzoyl}$), 137.3, 136.9, 133.1 ($C_{q\text{-}arom}$), 129.9, 129.3, 129.1, 128.5, 128.4, 128.4, 128.3, 128.1, 128.0, 126.2 (CH^{arom}), 101.5 (CHPh), 88.7 (C-1), 79.3 (C-2), 78.8 (C-3), 75.5 (CH_2 Bn), 75.1 (C-3), 70.6 (C-5), 68.8 (C-6). HRMS (ESI): $[M+Na]^+$ calcd for $C_{33}H_{30}O_6SNa$ 577.1655, found 577. 1649.

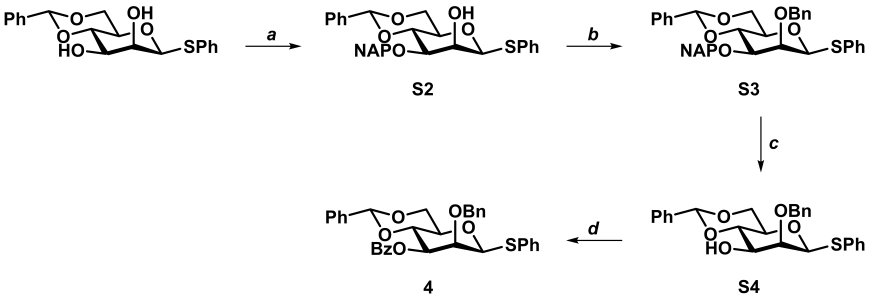

Supplementary scheme S2. Mannoside donor **4** synthesis. *Reagents and conditions:* a) 1. Dibutyltin(IV) oxide, toluene, reflux; 2. 2-(bromomethyl)naphthalene, CsF, DMF, **S2**: 49%; b) BnBr, NaH, DMF, 0 °C to RT, **S3**: quant.; c) DDQ, DCM:H_2O, **S4**: 87%; d) benzoyl chloride, pyridine, RT, **4**: 69%,.

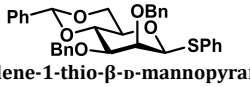

Phenyl 2,3-di-*O*-benzyl-4,6-*O*-benzylidene-1-thio-β-D-mannopyranoside (3). The title compound was prepared according to literature procedure.[11]

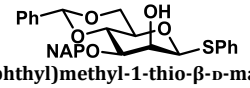

Phenyl 4,6-*O*-benzylidene-3-*O*-(2-naphthyl)methyl-1-thio-β-D-mannopyranoside (S2). The synthesis of **S2** started from phenyl 4,6-*O*-benzylidene-1-thio-β-D-mannopyranoside[11] (0.771 g, 2.14 mmol). Traces of solvent were removed from the glycoside by co-evaportation with toluene, and subsequently dissolved in toluene (8 ml, 0.3 M). Dibutyltin oxide (0.639 g, 2.57 mmol, 1.2 equiv) was added, and the resulting suspension was heated with an oil bath and refluxed for 1.5 h. The reaction mixture was concentrated *in vacuo*, coevaporated twice with toluene and dissolved in DMF (6 ml, 0.4 M). 2-(bromomethyl)naphthalene (0.709, 3.21 mmol, 1.5 equiv) and cesium fluoride (0.487, 3.21 mmol, 1.5 equiv) were added and it was stirred for 17 h. The reaction mixture was diluted with DCM and washed with sat. aq. $NaHCO_3$. The resulting tin paste was filtered from the solution using a Buchner funnel, and the filtrate was dried over $MgSO_4$. It was filtered off, and concentrated *in vacuo* to yield a white powder. Recrystalization from boiling EtOAc yielded the title compound (0.508 g, 1.044 mmol, 49%) as a white solid. TLC: R_f 0.25, (80:20, pentane:EtOAc, v:v); ^{1}H NMR (400 MHz, DMSO-d_6, HH-COSY, HSQC, HMBC) δ 7.94 – 7.18 (m, 17H, CH_{arom}), 5.71 (s, 1H, C*H*Ph), 5.68 (d, J = 6.1 Hz, 1H, 2-OH), 5.29 (d, J = 1.1 Hz, 1H, H-1), 4.88 (d, J = 12.9 Hz, 1H, C*H*H Nap), 4.77 (d, J = 13.0 Hz, 1H, C*H*H Nap), 4.31 (ddd, J = 6.0, 3.3, 1.3 Hz, 1H, H-2), 4.21 (dd, J = 10.2, 4.9 Hz, 1H, H-6), 4.08 (t, J = 9.6 Hz, 1H, H-4), 3.84 – 3.75 (m, 2H, H-3, H-6), 3.54 (td, J = 9.8, 4.9 Hz, 1H, H-5); ^{13}C{^{1}H} NMR (101 MHz, DMSO-d_6, HSQC, HMBC) δ 137.9, 136.5, 135.9, 132.8, 132.4 ($C_{q\text{-}arom}$), 129.1, 128.8, 128.5, 128.1, 127.6, 127.6, 126.2, 126.1, 126.1, 125.8, 125.7, 125.6 (CH_{arom}), 100.6 (CHPh), 87.2 (C-1), 78.0 (C-3), 77.2 (C-4), 70.4 (C-5), 70.1 (CH_2 Nap), 69.7 (C-2), 67.8 (C-6); HRMS (ESI): $[M+NH4]^+$ calcd for $C_{30}H_{28}O_5SNH4$ 518.1996, found 518.1998.

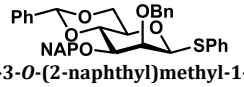

Pheny 2-*O*-benzyl-4,6-*O*-benzylidene-3-*O*-(2-naphthyl)methyl-1-thio-β-D-mannopyranoside (S3). S2 (0.508 g, 1.04 mmol) was dissolved in dry DMF (5 ml, 0.2M) and cooled to 0 °C. Under inert atmosphere, NaH (60 Wt % dispersion in mineral oil, 0.063 g, 1.57 mmol, 1.5 equiv) was added portion wise and the reaction mixture was stirred for 10 minutes. Benzyl bromide (0.155 ml, 1.31 mmol, 1.25 equiv) was added and the reaction was stirred for 17 h while allowing to warm up to RT. Subsequently, the reaction was cooled to 0 °C and quenched with H_2O. The reaction mixture was diluted with H_2O and extracted with DCM. The organic layers were combined, washed with brine, dried over $MgSO_4$ and concentrated *in vacuo*. Flash column chromatography (100:0 → 90:10, pentane:EtOAc v:v) yielded the title compound (0.613 g, quant) as a white solid. TLC: R_f 0.39, (90:10, pentane:EtOAc, v:v); ^{1}H NMR (500 MHz, $CDCl_3$, HH-COSY, HSQC, HMBC) δ 7.90 – 7.12 (m, 29H, CH_{arom}), 5.66 (s, 1H, C*H*Ph), 5.15 (d, J = 11.1 Hz, 1H, C*H*H NAP), 5.02 (d, J = 12.6 Hz, 1H, C*H*H Bn), 4.93 – 4.87 (m, 2H, CH*H* Bn, CH*H* NAP), 4.84 (d, J = 1.3 Hz, 1H, H-1), 4.39 – 4.26 (m, 2H, H-4, H-6), 4.19 (dd, J = 3.1, 1.3 Hz, 1H, H-2), 3.95 (t, J = 10.3 Hz, 1H, H-6), 3.78 (dd, J = 9.8, 3.1 Hz, 1H, H-3), 3.42 (ddd, J = 10.1, 9.2, 4.9 Hz, 1H, H-5); ^{13}C{^{1}H} NMR (126 MHz, $CDCl_3$, HSQC, HMBC) δ 138.1, 137.7, 135.8, 135.1, 133.4, 133.1 ($C_{q\text{-}arom}$), 131.3, 129.1, 129.1, 128.8, 128.4, 128.4, 128.1, 127.9, 127.8, 127.6, 126.6, 126.3, 126.1, 125.8 (CH_{arom}), 101.7 (CHPh),

89.3 (C-1), 79.7 (C-3), 79.0 (C-2), 78.8 (C-3), 76.1 (CH_2 NAP), 73.3 (CH_2 Bn), 71.9 (C-5), 68.6 (C-6). HRMS (ESI): $[M+NH4]^+$ calcd for $C_{37}H_{34}O_5SNH4$ 608.2465, found 608.2463.

Phenyl 2-*O*-benzyl-4,6-*O*-benzylidene-1-thio-β-D-mannopyranoside (S4). S3 (0.538 g, 0.910 mmol) was dissolved in DCM:H_2O (9:1, v:v, 5.5 ml, 0.2M), after which 2,3-Dichloro-5,6-dicyano-1,4-benzoquinone (0.310 g, 1,37 mmol, 1.5 equiv) was added. The reaction was protected from light and stirred for 1.5 h. The reaction was quenched by addition of sat. aq. $Na_2S_3O_3$ and filtered. The bi-phasic mixture was extracted with DCM. The organic layers were combined and washed with sat. aq. $NaHCO_3$, dried over $MgSO_4$, filtered and concentrated *in vacuo*. Flash column chromatography (90:10 → 80:20, pentane:EtOAc v:v) yielded the title compound (0.355 g, 0.788 mmol, 87%) as a white solid. TLC: R_f 0.40, (80:20, pentane:EtOAc, v:v); ^{1}H NMR (400 MHz, $CDCl_3$, HH-COSY, HSQC) δ 7.70 – 7.11 (m, 15H, CH_{arom}), 5.56 (s, 1H, C*H*Ph), 5.08 – 4.85 (m, 3H, H-1, C*H*H Bn, CH*H* Bn), 4.31 (dd, J = 10.5, 5.0 Hz, 1H, H-6), 4.15 (dd, J = 3.5, 1.3 Hz, 1H, H-2), 3.99 (t, J = 9.5 Hz, 1H, H-4), 3.94 – 3.81 (m, 2H, H-3, H-6), 3.41 (ddd, J = 10.2, 9.1, 5.0 Hz, 1H, H-5), 2.45 (d, J = 5.9 Hz, 1H, OH); ^{13}C{^{1}H} NMR (101 MHz, $CDCl_3$, HSQC, HMBC) δ 137.9, 137.3, 134.8 ($C_{q\text{-}arom}$), 131.3, 129.4, 129.2, 128.6, 128.6, 128.5, 128.2, 127.7, 126.4 (CH_{arom}), 102.2 (CHPh), 89.0 (C-1), 80.6 (C-2), 78.8 (C-4), 76.8 (CH_2 Bn), 73.0 (C-3), 71.3 (C-5), 68.5 (C-6); HRMS (ESI): $[M+Na]^+$ calcd for $C_{26}H_{26}O_5SNa$ 473.1393, found 473.1392.

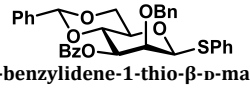

Phenyl 3-*O*-benzoyl-2-*O*-benzyl-4,6-*O*-benzylidene-1-thio-β-D-mannopyranoside (4). S4 (0.309 g, 0.686 mmol) was dissolved in pyridine (1.5 ml, 0.5 M), benzoyl chloride (0.145 g, 0.120 ml, 1.03 mmol, 1.5 equiv) was added and the reaction was stirred for 4 hours. It was diluted with ethyl acetate and sequentially washed with 1M HCl (aq.) and sat. aq. $NaHCO_3$. The organic layers were combined, dried over $MgSO_4$, filtered and concentrated *in vacuo*. Flash column chromatography (100:0 → 90:10, pentane:EtOAc v:v) yielded the title compound 0.261 g, 0.470 mmol, 69 %) as a white foam. TLC: R_f 0.40, (90:10, pentane:EtOAc, v:v); ^{1}H NMR (500 MHz, $CDCl_3$, HH-COSY, HSQC, HMBC) δ 8.19 – 7.14 (m, 20H), 5.62 (s, 1H, C*H*Ph), 5.36 (dd, *J* = 10.3, 3.3 Hz, 1H, H-3), 5.06 (d, *J* = 1.3 Hz, 1H, H-1), 4.81 (d, *J* = 11.0 Hz, 1H, C*H*H Bn), 4.77 (d, *J* = 10.9 Hz, 1H, CH*H* Bn), 4.49 (dd, *J* = 3.4, 1.3 Hz, 1H, H-2), 4.41 (dd, *J* = 10.3, 9.3 Hz, 1H, H-6), 4.35 (dd, *J* = 10.6, 4.9 Hz, 1H, H-4), 3.98 (t, *J* = 10.3 Hz, 1H, H-6), 3.60 (td, *J* = 9.9, 4.9 Hz, 1H, H-5); ^{13}C{^{1}H} NMR (126 MHz, $CDCl_3$, HSQC, HMBC) δ 166.2 ($C_{q\text{-}benzoyl}$), 137.5, 137.3, 134.5 ($C_{q\text{-}arom}$), 133.5, 131.7, 130.1 (CH_{arom}), 129.6 ($C_{q\text{-}arom}$), 129.2, 129.1, 128.6, 128.4, 128.4, 128.3, 128.0, 127.9, 126.2 (CH_{arom}), 101.8 (CHPh), 89.2 (C-1), 78.8 (C-2), 76.6 (CH_2 Bn), 75.7 (C-4), 74.4 (C-3), 71.9 (C-5), 68.6 (C-6). HRMS (ESI): $[M+Na]^+$ calcd for $C_{33}H_{30}O_6SNa$ 577.1655, found 577.1651.

Model glycosylations S5-S19

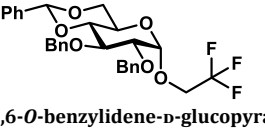

2,2,2-Trifluoroethyl 2,3-di-*O*-benzyl-4,6-*O*-benzylidene-D-glucopyranoside (S5). The title compound was prepared according the general glycosylation protocol, using **1** as the donor and 2,2,2-trifluoroethanol as the acceptor. Flash column chromatography (100:0 → 90:10, pentane:EtOAc v:v) yielded the title compound (39 mg, 0.074 mmol, 74%, α:β; 95:5) as a colorless oil. TLC: R_f 0.42, (90:10, pentane:EtOAc, v:v); ^{1}H NMR (850 MHz, $CDCl_3$, HH-COSY, HSQC, HMBC, HMBC-Gated) and ^{13}C{^{1}H} NMR (214 MHz, $CDCl_3$, HSQC, HMBC, HMBC-Gated) were in accordance to literature[11]; HRMS (ESI) M/Z: $[M + Na]^+$ Calcd for $C_{29}H_{29}F_3O_6Na$ 553.1808; Found 553.1804.

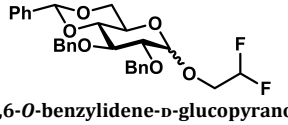

2,2-Difluoroethyl 2,3-di-*O*-benzyl-4,6-*O*-benzylidene-D-glucopyranoside (S6). The title compound was prepared according the general glycosylation protocol, using **1** as the donor and 2,2-difluoroethanol as the acceptor. Flash column chromatography (100:0 → 85:15, pentane:EtOAc v:v) yielded the title compound (40 mg, 0.095 mmol, 95%, α:β; 82:18) as a colorless oil. TLC: R_f 0.33, (90:10, pentane:EtOAc, v:v); ^{1}H NMR (850 MHz, $CDCl_3$, HH-COSY, HSQC, HMBC, HMBC-Gated) and ^{13}C{^{1}H} NMR (214 MHz, $CDCl_3$, HSQC, HMBC, HMBC-Gated) were in accordance to literature[11]; HRMS (ESI) M/Z: $[M + Na]^+$ Calcd for $C_{29}H_{30}F_2O_6Na$ 535.1903; Found 535.1902.

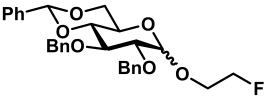

2-Fluoroethyl 2,3-di-*O*-benzyl-4,6-*O*-benzylidene-D-glucopyranoside (S7). The title compound was prepared according the general glycosylation protocol, using **1** as the donor and 2-fluoroethanol as the acceptor. Flash column chromatography (95:5 → 80:20, pentane:EtOAc v:v) yielded the title compound (32 mg, 0.065 mmol, 65%, α:β; 50:50) as a colorless oil. TLC: R_f 0.20, (90:10, pentane:EtOAc, v:v); ^{1}H NMR (850 MHz, $CDCl_3$, HH-COSY, HSQC, HMBC, HMBC-Gated) and $^{13}C\{^1H\}$ NMR (214 MHz, $CDCl_3$, HSQC, HMBC, HMBC-Gated) were in accordance to literature[11]; HRMS (ESI) M/Z: $[M + Na]^+$ Calcd for $C_{29}H_{31}FO_6Na$ 517.1997; Found 517.1996.

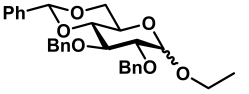

Ethyl 2,3-di-*O*-benzyl-4,6-*O*-benzylidene-D-glucopyranoside (S8). The title compound was prepared according the general glycosylation protocol, using **1** as the donor and ethanol as the acceptor. Flash column chromatography (100:0 → 90:10, pentane:EtOAc v:v) yielded the title compound (48 mg, 0.080 mmol, 80%, α:β; 30:70) as a colorless oil. TLC: R_f 0.51, (90:10, pentane:EtOAc, v:v); ^{1}H NMR (850 MHz, $CDCl_3$, HH-COSY, HSQC, HMBC, HMBC-Gated) and $^{13}C\{^1H\}$ NMR (214 MHz, $CDCl_3$, HSQC, HMBC, HMBC-Gated) were in accordance to literature[11]; HRMS (ESI) M/Z: $[M + Na]^+$ Calcd for $C_{29}H_{32}O_6Na$ 499.2091; Found 499.2090.

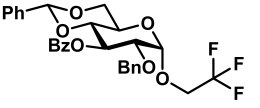

2,2,2-Trifluoroethyl 3-*O*-benzoyl-2-*O*-benzyl-4,6-*O*-benzylidene-D-glucopyranoside (S9). The title compound was prepared according the general glycosylation protocol, using **2** as the donor and 2,2,2-trifluoroethanol as the acceptor. Flash column chromatography (100:0 → 90:10, pentane:EtOAc v:v) yielded the title compound (46 mg, 0.084 mmol, 84%, α:β; >98:2) as a colorless oil. TLC: R_f 0.18, (90:10, pentane:EtOAc, v:v); ^{1}H NMR (850 MHz, $CDCl_3$, HH-COSY, HSQC, HMBC, HMBC-Gated) δ 8.11 – 7.19 (m, 15H, CH_{arom}), 5.84 (t, *J* = 9.7 Hz, 1H, H-3), 5.47 (s, 1H, C*H*Ph), 4.91 (d, *J* = 3.7 Hz, 1H, H-1), 4.64 (d, *J* = 12.5 Hz, 1H, C*H*H Bn), 4.59 (d, *J* = 12.4 Hz, 1H, CH*H* Bn), 4.28 (dd, *J* = 10.5, 4.9 Hz, 1H, H-6), 4.03 – 3.89 (m, 3H, H-5, C*H*HCF$_3$, CH*H*CF$_3$), 3.80 – 3.68 (m, 3H, H-2, H-4, H-6); $^{13}C\{^1H\}$ NMR (214 MHz, $CDCl_3$, HSQC, HMBC, HMBC-Gated) δ 165.5 ($C_{q\text{-}benzoyl}$), 137.5, 136.9 ($C_{q\text{-}arom}$), 133.1, 131.2 (CH_{arom}), 130.1 ($C_{q\text{-}arom}$), 129.9, 129.5, 129.1, 128.6, 128.5, 128.3, 128.2, 128.1, 126.2, 124.9 (CH_{arom}), 123.69 (q, *J* = 278.9 Hz, CF_3), 101.6 (CHPh), 98.5 (C-1), 79.3 (C-4), 77.1 (C-2), 72.9 (CH_2 Bn), 70.8 (C-3), 68.8 (C-6), 65.31 (dd, *J* = 70.3, 35.1 Hz, CH_2CF_3), 63.3 (C-5); ^{13}C-GATED NMR (214 MHz, $CDCl_3$) δ 98.5 ($J_{H1\text{-}C1}$ = 169 Hz, α); HRMS (ESI) M/Z: $[M + Na]^+$ Calcd for $C_{29}H_{27}F_3O_7Na$ 567.1601; Found 567.1599.

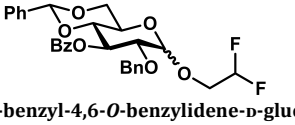

2,2-Difluoroethyl 3-*O*-benzoyl-2-*O*-benzyl-4,6-*O*-benzylidene-D-glucopyranoside (S10). The title compound was prepared according the general glycosylation protocol, using **2** as the donor and 2,2-difluoroethanol as the acceptor. Flash column chromatography (100:0 → 85:15, pentane:EtOAc v:v) yielded the title compound (39 mg, 0.074 mmol, 74%, α:β; 85:15) as a colorless oil. TLC: R_f 0.13, (90:10, pentane:EtOAc, v:v); Spectroscopic data for the major anomer: ^{1}H NMR (850 MHz, $CDCl_3$, HH-COSY, HSQC, HMBC, HMBC-Gated) δ 8.20 – 6.83 (m, 15H, CH_{arom}), 5.99 (tdd, *J* = 55.5, 4.7, 3.9 Hz, 1Hz, CHF_2), 5.83 (t, *J* = 9.7 Hz, 1H, H-3), 5.47 (s, 1H, C*H*Ph), 4.88 (d, *J* = 3.7 Hz, 1H, H-1), 4.63 (d, *J* = 12.3 Hz, 1H, C*H*H Bn), 4.59 (d, *J* = 12.4 Hz, 1H, CH*H* Bn), 4.29 (dd, *J* = 10.4, 4.9 Hz, 1H, H-6), 3.99 (td, *J* = 9.9, 4.9 Hz, 1H, H-5), 3.90 – 3.70 (m, 5H, H-2, H-4, H-6, C*H*HCHF$_2$, CH*H*CHF$_2$); $^{13}C\{^1H\}$ NMR (214 MHz, $CDCl_3$, HSQC, HMBC, HMBC-Gated) δ 165.5 ($C_{q\text{-}benzoyl}$), 137.5, 136.9 ($C_{q\text{-}arom}$), 133.2, 131.2 (CH_{arom}), 130.1 ($C_{q\text{-}arom}$), 130.0, 129.4, 129.1, 128.6, 128.5, 128.4, 128.3, 128.2, 128.1, 126.2, 124.9 (CH_{arom}), 114.2 (t, *J* = 241.4 Hz, CHF_2), 101.6 (CHPh), 98.4 (C-1), 79.4 (C-4), 77.3 (C-2), 73.0 (CH_2 Bn), 70.9 (C-3), 68.9 (C-6), 67.5 (t, J = 29.0 Hz, CH_2CHF_2), 63.1 (C-5); ^{13}C-GATED NMR (214 MHz, $CDCl_3$) δ 98.4 ($J_{H1\text{-}C1}$ = 173 Hz, α); Diagnostic peaks for the minor anomer: ^{1}H NMR (850 MHz, $CDCl_3$, HH-COSY, HSQC, HMBC, HMBC-Gated) δ 5.95 (tdd, *J* = 55.0, 4.8, 3.3 Hz, 1H, CHF_2), 4.79 (d, *J* = 11.6 Hz, 1H, C*H*H Bn), 4.70 (d, *J* = 7.5 Hz, 1H, H-1), 4.37 (dd, *J* = 10.6, 5.0 Hz, 1H, H-6), 3.63 – 3.56 (m, 2H, H-2, H-5); $^{13}C\{^1H\}$ NMR (214 MHz, $CDCl_3$, HSQC, HMBC, HMBC-Gated) δ 165.6 ($C_{q\text{-}benzoyl}$), 137.4, 136.8 ($C_{q\text{-}arom}$), 104.5 (C-1), 101.5 (CHPh), 79.1 (C-4), 78.7 (C-2), 74.5 (CH_2 Bn), 68.7 (C-6), 66.4 (C-5); ^{13}C-GATED NMR (214 MHz, $CDCl_3$) δ 104.5 ($J_{H1\text{-}C1}$ = 163 Hz, β); HRMS (ESI) M/Z: $[M + Na]^+$ Calcd for $C_{29}H_{28}F_2O_7Na$ 549.1695; Found 549.1693.

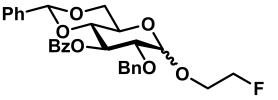

2-Fluoroethyl 3-*O*-benzoyl-2-*O*-benzyl-4,6-*O*-benzylidene-D-glucopyranoside (S11). The title compound was prepared according the general glycosylation protocol, using **2** as the donor and 2-fluoroethanol as the acceptor. Flash column chromatography (95:5 → 80:20, pentane:EtOAc v:v) yielded the title compound (quant, α:β; 45:55) as a colorless oil. TLC: R_f 0.06, (90:10, pentane:EtOAc, v:v); Spectroscopic data reported as a mixture of anomers: ^{1}H NMR (850 MHz, $CDCl_3$, HH-COSY, HSQC, HMBC, HMBC-Gated) δ 8.08 – 7.08 (m, 30H, CH_{arom}), 5.86 (t, *J* = 9.7 Hz, 1H, H-3 α), 5.59 (dd, *J* = 9.7, 9.1 Hz, 1H, H-3 β), 5.47 (s, 2H, C*H*Ph α, C*H*Ph β), 4.94 (d, *J* = 3.6 Hz, 1H, H-1 α), 4.83 (d, *J* = 11.6 Hz, 1H, C*H*H Bn β), 4.71 (d, *J* = 7.6 Hz, 1H, H-1 β), 4.69 – 4.58 (m, 7H, C*H*H Bn α, CH*H* Bn α, CH*H* Bn β, C*H*HF α, CH*H*F α, C*H*HF β, CH*H*F β), 4.37 (dd, *J* = 10.6, 5.0 Hz, 1H, H-6 β), 4.29 (dd, *J* = 10.4, 5.0 Hz, 1H, H-6 α), 4.14 (dddd, *J* = 31.8, 12.1, 5.1, 2.3 Hz, 1H, C*H*HCH$_2$F β), 4.04 (td, *J* = 9.9, 4.9 Hz, 1H, H-5 α), 3.95 – 3.85 (m, 2H, CH*H*CH$_2$F α, CH*H*CH$_2$F β), 3.84 – 3.76 (m, 2H, H-6 β, CH*H*CH$_2$F α), 3.76 – 3.69 (m, 4H, H-2 α, H-4 α, H-6 α, H-4 β), 3.61 (dd, *J* = 9.1, 7.5 Hz, 1H, H-2 β), 3.58 (td, *J* = 9.8, 5.0 Hz, 1H, H-5 β); ^{13}C{^{1}H} NMR (214 MHz, $CDCl_3$, HSQC, HMBC, HMBC-Gated) δ 165.6 ($C_{q\text{-benzoyl}}$ β), 165.5 ($C_{q\text{-benzoyl}}$ α), 145.6, 137.7, 137.6, 137.0, 136.9 ($C_{q\text{-arom}}$), 133.1, 133.0, 131.2jjjj, 130.2, 130.0 (CH_{arom}), 130.0, 129.9 ($C_{q\text{-arom}}$), 129.4, 129.1, 129.0, 128.5, 128.5, 128.4, 128.4, 128.3, 128.3, 128.2, 128.1, 128.0, 127.8, 126.2, 126.2, 124.9 (CH_{arom}), 104.4 (C-1 β), 101.5 (CHPh α), 101.4 (CHPh β), 98.0 (C-1 α), 82.5 (d, *J* = 170.3 Hz, CH_2F β), 82.8 (d, *J* = 170.0 Hz, CH_2F α), 79.6 (C-2 α), 79.1 (C-2 β), 78.8 (C-4 β), 77.4 (C-4 α), 74.4 (CH_2 Bn β), 73.1 (C-3 β), 72.7(CH_2 Bn α), 71.1 (C-3 α), 69.4 (d, *J* = 19.9 Hz, CH_2CH_2F β), 69.0 (C-6 α), 68.8 (C-6 β), 67.5 (d, *J* = 20.1 Hz, CH_2CH_2F α), 66.3 (C-5 β), 62.7 (C-5 α); HRMS (ESI) M/Z: $[M + Na]^+$ Calcd for $C_{29}H_{29}FO_7Na$ 531.1790; Found 531.1788.

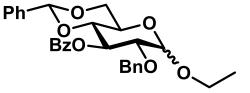

Ethyl 3-*O*-benzoyl-2-*O*-benzyl-4,6-*O*-benzylidene-D-glucopyranoside (S12). The title compound was prepared according the general glycosylation protocol, using **2** as the donor and ethanol as the acceptor. Flash column chromatography (100:0 → 90:10, pentane:EtOAc v:v) yielded the title compound (quant, α:β; 25:75) as a colorless oil. TLC: R_f 0.21, (90:10, pentane:EtOAc, v:v); Spectroscopic data for the major anomer: ^{1}H NMR (850 MHz, $CDCl_3$, HH-COSY, HSQC, HMBC, HMBC-Gated) δ 8.14 – 7.03 (m, 15H, CH_{arom}), 5.58 (t, *J* = 9.5 Hz, 1H, H-3), 5.47 (s, 1H, C*H*Ph), 4.82 (d, *J* = 11.7 Hz, 1H, C*H*H Bn), 4.68 – 4.65 (m, 2H, H-1, C*H*H Bn), 4.63, 4.37 (dd, *J* = 10.6, 5.0 Hz, 1H, H-6), 4.06 – 3.99 (m, 1H, C*H*HCH$_3$), 3.80 (t, *J* = 10.3 Hz, 1H, H-6), 3.78 – 3.67 (m, 2H, H-4, H-5), 3.59 – 3.55 (m, 2H, H-2, CH*H*CH$_3$), 1.32 (t, *J* = 7.1 Hz, 3H, CH_3); ^{13}C{^{1}H} NMR (214 MHz, $CDCl_3$, HSQC, HMBC, HMBC-Gated) δ 165.6 ($C_{q\text{-benzoyl}}$), 137.7, 137.0 ($C_{q\text{-arom}}$), 133.1 (CH_{arom}), 130.1 ($C_{q\text{-arom}}$), 130.0, 129.1, 128.4, 128.4, 128.3, 128.3, 127.7, 126.2 (CH_{arom}), 104.2 (C-1), 101.4 (CHPh), 79.4 (C-2), 79.0 (C-4), 74.4 (CH_2 Bn), 73.2 (C-3), 68.9 (C-6), 66.3 (C-5), 66.3 (CH_2CH_3), 15.5 (CH_3); Spectroscopic data for the minor anomer: ^{1}H NMR (850 MHz, $CDCl_3$, HH-COSY, HSQC, HMBC, HMBC-Gated) δ 8.14 – 7.03 (m, 15H, CH_{arom}), 5.86 (t, *J* = 9.7 Hz, 1H, H-3), 5.47 (s, 1H, C*H*Ph), 4.86 (d, *J* = 3.6 Hz, 1H, H-1), 4.64 (d, *J* = 12.5 Hz, 1H, C*H*H Bn), 4.60 (d, *J* = 12.5 Hz, 1H, CH*H* Bn), 4.28 (dd, *J* = 10.4, 4.9 Hz, 1H, H-6), 4.06 – 3.99 (m, 1H, H-5), 3.78 – 3.67 (m, 4H, H-2, H-4, H-6, C*H*HCH$_3$), 3.53 (dq, *J* = 9.7, 7.0 Hz, 1H, C*H*HCH$_3$), 1.30 (t, *J* = 7.1 Hz, 3H, CH_3); ^{13}C{^{1}H} NMR (214 MHz, $CDCl_3$, HSQC, HMBC-Gated) δ 165.5 ($C_{q\text{-benzoyl}}$), 137.8, 137.1, 133.1 ($C_{q\text{-arom}}$), 133.0 (CH_{arom}), 130.3 ($C_{q\text{-arom}}$), 129.9, 129.0, 128.5, 128.4, 128.2, 128.0, 126.2 (CH_{arom}), 101.5 (CHPh), 97.5 (C-1), 79.9 (C-2), 77.5 (C-4), 72.7 (CH_2 Bn), 71.3 (C-3), 69.1 (C-6), 64.0 (CH_2CH_3), 62.6 (C-5), 15.5 (CH_3); HRMS (ESI) M/Z: $[M + Na]^+$ Calcd for $C_{29}H_{30}O_7Na$ 513.1884; Found 513.1880.

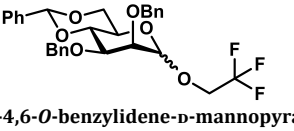

2,2,2-Trifluoroethyl 2,3-di-*O*-benzyl-4,6-*O*-benzylidene-D-mannopyranoside (S13). The title compound was prepared according the general glycosylation protocol, using **3** as the donor and 2,2,2-trifluoroethanol as the acceptor. Flash column chromatography (100:0 → 90:10, pentane:EtOAc v:v) yielded the title compound (27 mg, 0.051 mmol, 51%, α:β; 23:77) as a colorless oil. TLC: R_f 0.52, (90:10, pentane:EtOAc, v:v); ^{1}H NMR (850 MHz, $CDCl_3$, HH-COSY, HSQC, HMBC, HMBC-Gated) and ^{13}C{^{1}H} NMR (214 MHz, $CDCl_3$, HSQC, HMBC-Gated) were in accordance to literature[11]; HRMS (ESI) M/Z: $[M + Na]^+$ Calcd for $C_{29}H_{29}F_3O_6Na$ 553.1808; Found 553.1805.

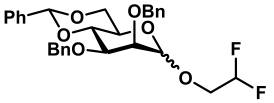

2,2-Difluoroethyl 2,3-di-*O*-benzyl-4,6-*O*-benzylidene-D-mannopyranoside (S14). The title compound was prepared according the general glycosylation protocol, using **3** as the donor and 2,2-difluoroethanol as the acceptor. Flash column chromatography (100:0 → 85:15, pentane:EtOAc v:v) yielded the title compound (30 mg, 0.059 mmol, 59%, α:β; 18:82) as a colorless oil. TLC: R_f 0.34, (90:10, pentane:EtOAc, v:v); ^{1}H NMR (850 MHz, $CDCl_3$, HH-COSY, HSQC, HMBC, HMBC-Gated) and $^{13}C\{^1H\}$ NMR (214 MHz, $CDCl_3$, HSQC, HMBC-Gated) were in accordance to literature[11]; HRMS (ESI) M/Z: $[M + Na]^+$ Calcd for $C_{29}H_{30}F_2O_6Na$ 535.1903; Found 535.1902.

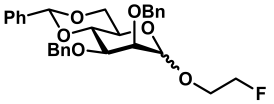

2-Fluoroethyl 2,3-di-*O*-benzyl-4,6-*O*-benzylidene-D-mannopyranoside (S15). The title compound was prepared according the general glycosylation protocol, using **3** as the donor and 2-fluoroethanol as the acceptor. Flash column chromatography (95:5 → 80:20, pentane:EtOAc v:v) yielded the title compound (30 mg, 0.061 mmol, 61%, α:β; 17:83) as a colorless oil. TLC: R_f 0.17, (90:10, pentane:EtOAc, v:v); ^{1}H NMR (850 MHz, $CDCl_3$, HH-COSY, HSQC, HMBC, HMBC-Gated) and $^{13}C\{^1H\}$ NMR (214 MHz, $CDCl_3$, HSQC, HMBC-Gated) were in accordance to literature[11]; HRMS (ESI) M/Z: $[M + Na]^+$ Calcd for $C_{29}H_{31}FO_6Na$ 517.1997; Found 517.1997.

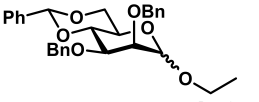

Ethyl 2,3-di-*O*-benzyl-4,6-*O*-benzylidene-D-mannopyranoside (S16). The title compound was prepared according the general glycosylation protocol, using **3** as the donor and ethanol as the acceptor. Flash column chromatography (100:0 → 90:10, pentane:EtOAc v:v) yielded the title compound (26 mg, 0.055 mmol, 55%, α:β; 19:81) as a colorless oil. TLC: R_f 0.42, (90:10, pentane:EtOAc, v:v); ^{1}H NMR (850 MHz, $CDCl_3$, HH-COSY, HSQC, HMBC, HMBC-Gated) and $^{13}C\{^1H\}$ NMR (214 MHz, $CDCl_3$, HSQC, HMBC-Gated) were in accordance to literature[11]; HRMS (ESI) M/Z: $[M + Na]^+$ Calcd for $C_{29}H_{32}O_6Na$ 499.2091; Found 499.2088.

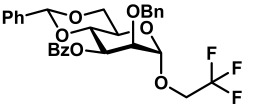

2,2,2-Trifluoroethyl 3-*O*-benzoyl-2-*O*-benzyl-4,6-*O*-benzylidene-D-mannopyranoside (S17). The title compound was prepared according the general glycosylation protocol, using **4** as the donor and 2,2,2-trifluoroethanol as the acceptor. Flash column chromatography (100:0 → 90:10, pentane:EtOAc v:v) yielded the title compound (45 mg, 0.083 mmol, 83%, α:β; >98:2) as a colorless oil. TLC: R_f 0.46, (90:10, pentane:EtOAc, v:v); ^{1}H NMR (850 MHz, $CDCl_3$, HH-COSY, HSQC, HMBC, HMBC-Gated) δ 8.09 – 7.19 (m, 15H, CH_{arom}), 5.62 (s, 1H, C*H*Ph), 5.56 (dd, J = 10.4, 3.6 Hz, 1H, H-3), 4.94 (d, J = 1.6 Hz, 1H, H-1), 4.65 (d, J = 12.0 Hz, 1H, C*H*H Bn), 4.62 (d, J = 11.9 Hz, 1H, CH*H* Bn), 4.37 (dd, J = 10.5, 9.4 Hz, 1H, H-4), 4.29 (dd, J = 10.2, 4.7 Hz, 1H, H-6), 4.18 (dd, J = 3.6, 1.6 Hz, 1H, H-2), 4.01 – 3.95 (m, 2H, H-5, C*H*HCF$_3$), 3.95 – 3.88 (m, 2H, CH*H*CF$_3$); $^{13}C\{^1H\}$ NMR (214 MHz, $CDCl_3$, HSQC, HMBC, HMBC-Gated) δ 165.8 ($C_{q\text{-benzoyl}}$), 137.2, 137.2 ($C_{q\text{-arom}}$), 133.3 (CH_{arom}), 130.0 ($C_{q\text{-arom}}$), 129.9, 128.7, 128.7, 128.6, 128.6, 128.5, 128.5, 128.4, 128.3, 128.2, 128.2, 128.1, 128.0, 126.2 (CH_{arom}), 123.6 (q, *J* = 278.6 Hz, CF_3), 101.9 (CHPh), 99.6 (C-1), 76.1 (C-4), 75.9 (C-2), 74.2 (CH_2 Bn), 70.7 (C-3), 68.6, (C-6) 64.9 (C-5), 64.55 (q, *J* = 35.2 Hz, CH_2CF_3); ^{13}C-GATED NMR (214 MHz, $CDCl_3$) δ 99.6 ($J_{H1\text{-}C1}$ = 172 Hz, α); HRMS (ESI) M/Z: $[M + Na]^+$ Calcd for $C_{29}H_{27}F_3O_7Na$ 567.1601; Found 567.1601.

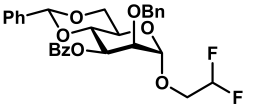

2,2-Difluoroethyl 3-*O*-benzoyl-2-*O*-benzyl-4,6-*O*-benzylidene-D-mannopyranoside (S18). The title compound was prepared according the general glycosylation protocol, using **4** as the donor and 2,2-difluoroethanol as the acceptor. Flash column chromatography (100:0 → 85:15, pentane:EtOAc v:v) yielded the title compound (38 mg, 0.072 mmol, 72%, α:β; >98:2) as a colorless oil. TLC: R_f 0.35, (90:10, pentane:EtOAc, v:v); ^{1}H NMR (850 MHz, $CDCl_3$, HH-COSY, HSQC, HMBC, HMBC-Gated) δ 8.10 – 7.15 (m, 15H, CH_{arom}), 5.92 (tdd, *J* = 55.4, 4.7, 3.6 Hz, 1H, CHF_2), 5.62 (s, 1H), 5.54 (dd, *J* = 10.4, 3.5 Hz, 1H, C*H*Ph), 4.91 (d, *J* = 1.6 Hz, 1H, H-3), 4.67 – 4.60 (m, 2H, C*H*H Bn, CH*H* Bn), 4.36 (dd, *J* = 10.5, 9.4 Hz, 1H, H-4), 4.29 (dd, *J* = 10.2, 4.7 Hz, 1H, H-6), 4.15 (dd, *J* = 3.5, 1.7 Hz, 1H, H-2), 3.97 (td, *J* = 9.9, 4.7 Hz, 1H, H-5), 3.91 (t, *J* = 10.3 Hz, 1H, H-6), 3.85 (dddd, *J* = 16.2, 12.9, 11.7, 3.7 Hz, 1H, C*H*HCHF$_2$), 3.72 (tdd, *J* = 12.7, 11.7, 4.7 Hz, 1H, CH*H*CHF$_2$); ^{13}C{^{1}H} NMR (214 MHz, $CDCl_3$, HSQC, HMBC, HMBC-Gated) δ 165.9 ($C_{q\text{-benzoyl}}$), 137.3, 137.3 ($C_{q\text{-arom}}$), 133.3, 130.0 (CH_{arom}), 129.9 ($C_{q\text{-arom}}$), 129.1, 128.6, 128.5, 128.3, 128.2, 128.1, 126.2 (CH_{arom}), 114.0 (t, *J* = 241.4 Hz, CHF_2), 101.8 (CHPh), 99.6 (C-1), 76.2 (C-4), 76.0 (C-2), 74.1 (CH_2 Bn), 70.9 (C-3), 68.7 (C-6), 66.8 (t, J = 28.6 Hz, CH_2CHF_2), 64.6 (C-5); ^{13}C-GATED NMR (214 MHz, $CDCl_3$) δ 99.6 ($J_{H1\text{-}C1}$ = 173 Hz, α); HRMS (ESI) M/Z: [M + Na]$^+$ Calcd for $C_{29}H_{28}F_2O_7Na$ 549.1695; Found 549.1697.

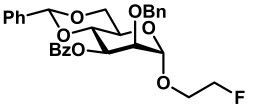

2-Fluoroethyl 3-*O*-benzoyl-2-*O*-benzyl-4,6-*O*-benzylidene-D-mannopyranoside (S19). The title compound was prepared according the general glycosylation protocol, using **4** as the donor and 2-fluoroethanol as the acceptor. Flash column chromatography (95:5 → 80:20, pentane:EtOAc v:v) yielded the title compound (48 mg, 0.094 mmol, 94%, α:β; >98:2) as a colorless oil. TLC: R_f 0.20, (90:10, pentane:EtOAc, v:v); ^{1}H NMR (850 MHz, $CDCl_3$, HH-COSY, HSQC, HMBC, HMBC-Gated) δ 8.15 – 7.17 (m, 15H, CH_{arom}), 5.62 (s, 1H, C*H*Ph), 5.60 (dd, *J* = 10.4, 3.5 Hz, 1H, H-3), 4.94 (d, *J* = 1.7 Hz, 1H, H-1), 4.66 – 4.63 (m, 2H, C*H*H Bn), 4.60 (dtdt, *J* = 10.6, 7.8, 4.9, 2.6 Hz, 1H, C*H*HF), 4.58 – 4.52 (m, 1H, CH*H*F), 4.36 (dd, *J* = 10.5, 9.4 Hz, 1H, H-4), 4.29 (dd, *J* = 10.3, 4.8 Hz, 1H, H-6), 4.15 (dd, *J* = 3.5, 1.7 Hz, 1H, H-2), 4.02 (td, *J* = 9.9, 4.8 Hz, 1H, H-5), 3.95 – 3.86 (m, 2H, H-6, C*H*HCH$_2$F), 3.75 (dddd, *J* = 27.0, 12.2, 6.3, 2.8 Hz, 1H, C*H*HCH$_2$F); ^{13}C{^{1}H} NMR (214 MHz, $CDCl_3$, HSQC, HMBC, HMBC-Gated) δ ^{13}C{^{1}H} NMR (214 MHz, $CDCl_3$) δ 165.9 ($C_{q\text{-benzoyl}}$), 145.6, 137.5 ($C_{q\text{-arom}}$), 137.3, 133.2, 131.2, 130.0 (CH_{arom}), 130.0 ($C_{q\text{-arom}}$), 129.4, 129.0, 128.5, 128.5, 128.3, 128.0, 128.0, 126.2, 124.9 (CH_{arom}), 101.8 (CHPh), 99.3 (C-1), 82.5 (d, *J* = 170.1 Hz, CH_2F), 76.4 (C-4), 76.4 (C-2), 73.9 (CH_2 Bn), 71.1 (C-3), 68.8 (C-6), 66.9 (d, *J* = 20.0 Hz, CH_2CH_2F), 64.3 (C-5); ^{13}C-GATED NMR (214 MHz, $CDCl_3$) δ 99.3 ($J_{H1\text{-}C1}$ = 171 Hz, α); HRMS (ESI) M/Z: [M + Na]$^+$ Calcd for $C_{29}H_{29}FO_7Na$ 531.1790; Found 531.1791.

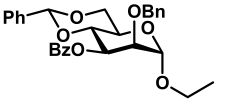

Ethyl 3-*O*-benzoyl-2-*O*-benzyl-4,6-*O*-benzylidene-D-mannopyranoside (S20). The title compound was prepared according the general glycosylation protocol, using **4** as the donor and ethanol as the acceptor. Flash column chromatography (100:0 → 90:10, pentane:EtOAc v:v) yielded the title compound (36 mg, 0.073 mmol, 73%, α:β; >98:2) as a colorless oil. TLC: R_f 0.48, (90:10, pentane:EtOAc, v:v); ^{1}H NMR (850 MHz, $CDCl_3$, HH-COSY, HSQC, HMBC, HMBC-Gated) δ 8.16 – 7.15 (m, 15H, CH_{arom}), 5.62 (s, 1H, C*H*Ph), 5.60 (dd, *J* = 10.4, 3.5 Hz, 1H, H-3), 4.87 (d, *J* = 1.7 Hz, 1Hz, H-1), 4.65 (s, 2H, CH_2 Bn), 4.34 (dd, *J* = 10.5, 9.4 Hz, 1H, H-4), 4.29 (dd, *J* = 10.3, 4.7 Hz, 1H, H-6), 4.08 (dd, *J* = 3.6, 1.7 Hz, 1H, H-2), 4.00 (td, *J* = 9.9, 4.7 Hz, 1H, H-5), 3.91 (t, *J* = 10.3 Hz, 1H, H-6), 3.77 (dq, *J* = 9.6, 7.1 Hz, 1H, C*H*HCH$_3$), 3.48 (dq, *J* = 9.6, 7.0 Hz, 1H, CH*H*CH$_3$), 1.23 (t, *J* = 7.1 Hz, 3H, CH_3); ^{13}C{^{1}H} NMR (214 MHz, $CDCl_3$, HSQC, HMBC, HMBC-Gated) δ 165.9 ($C_{q\text{-benzoyl}}$), 137.7, 137.4 ($C_{q\text{-arom}}$), 133.2 (CH_{arom}), 130.1 ($C_{q\text{-arom}}$), 129.0, 128.5, 128.5, 128.3, 128.0, 128.0, 126.2 (CH_{arom}), 101.8 (CHPh), 98.9 (C-1), 76.7 (C-2), 76.6 (C-4), 73.9 (CH_2 Bn), 71.3 (C-3), 69.0 (C-6), 64.1 (C-5), 63.5 (CH_2CH_3), 15.1 (CH_3); ^{13}C-GATED NMR (214 MHz, $CDCl_3$) δ 98.9 ($J_{H1\text{-}C1}$ = 170 Hz, α); HRMS (ESI) M/Z: [M + Na]$^+$ Calcd for $C_{29}H_{30}O_7Na$ 513.1884; Found 513.1884.

Preparation of the IR donors 5-6

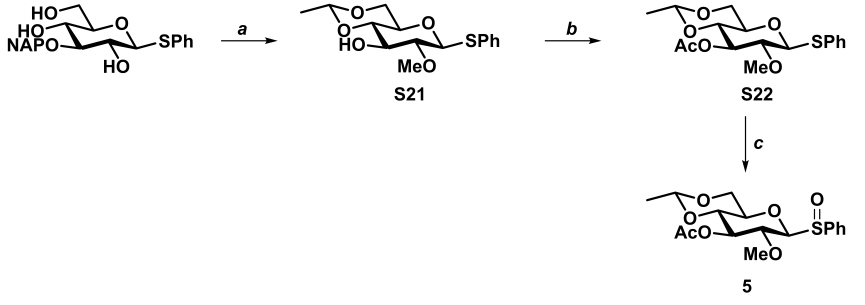

Supplementary scheme S3. Glucoside donor **5** synthesis. *Reagents and conditions:* a) 1. 1,1-dimethoxyethane, camphorsulfonic acid, acetonitril, RT, **2**. DDQ, DCM:H_2O, S21: 66%; b) acetic anhydride, pyridine, RT, **S22**: 63%; c) *meta*-chloroperoxybenzoic acid, DCM, **5**: quant.

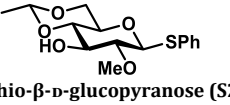

Phenyl 4,6-*O*-ethylidene-2-*O*-methyl-1-thio-β-D-glucopyranose (S21). To a solution of phenyl 2-O-methyl-3-O-(2-methyl)naphthyl-1-thio-β-d-glucopyranoside (50 mg, 0.12 mmol) in dry acetonitrile (1.2 ml, 0.1M) and 1,1-dimethoxyethane (0.033 ml, 0.35 mmol, 3 equiv), CSA (2.7 mg, 0.012 mmol, 0.1 equiv) was added. The mixture stirred under argon atmosphere for 16 hours before being quenched by addition of triethylamine (0.10 ml). The resulting solution was concentrated *in vacuo*, diluted with EtOAc and washed with sat. aq. $NaHCO_3$ and brine. The organic layer was dried over $MgSO_4$, filtered and concentrated *in vacuo*. To a solution of the crude phenyl 2-*O*-methyl-3-*O*-(2-methyl)naphthyl-4,6-*O*-ethylidene-1-thio-β-d-glucopyranoside (20 mg, 0.044 mmol) in DCM/H_2O (7/1, 0.5 ml, 0.1M) was added DDQ (15 mg, 0.066 mmol, 1.5 equiv) and the reaction mixture was stirred in the dark to completion. The reaction mixture was diluted using DCM (5 mL). The organic phase was washed twice using an aqueous mixture of ascorbic acid (0.7%), citric acid (1.5%) and NaOH (0.9%) (w/v). The organic layer way dried over $MgSO_4$, filtered and concentrated *in vacuo*. Flash column chromatography (100:0 → 70:30, *n*-heptane:EtOAc v:v) yielded the title compound (14 mg, 0.044 mmol, 66%) as a white amorphous solid. TLC: R_f 0.28, (50:50, *n*-heptane:EtOAc, v:v); ^{1}H NMR (500 MHz, $CDCl_3$) δ 7.56 – 7.46 (m, 2H, CH_{arom}), 7.37 – 7.26 (m, 3H, CH_{arom}), 4.72 (q, *J* = 5.0 Hz, 1H, CH_3CH), 4.61 (d, *J* = 9.8 Hz, 1H, H-1), 4.26 – 4.10 (m, 1H, H-6), 3.76 (ddt, *J* = 8.7, 5.8, 2.3 Hz, 1H, H-3), 3.67 (s, 1H, OCH_3), 3.63 – 3.44 (m, 1H, H-6), 3.35 – 3.20 (m, 2H, H-4, H-5), 3.11 (dd, *J* = 9.7, 8.4 Hz, 1H, H-2), 2.70 (d, *J* = 2.5 Hz, 1H, 3-O*H*), 1.36 (d, *J* = 5.0 Hz, 3H, CH_3CH); ^{13}C{^{1}H} NMR (126 MHz, $CDCl_3$) δ 133.2, 132.2, 129.1, 128.0 (CH_{arom}), 99.8 (CH_3CH), 87.8 (C-1), 82.8 (C-2), 79.7 (C-4), 75.5 (C-3), 70.3 (C-5), 68.3 (C-6), 61.5 (OCH_3), 20.4 (CH_3CH); HRMS (ESI): $[M + Na]^+$ Calcd. for $C_{15}H_{20}O_5SNa$ 335.0929, found 335.09332.

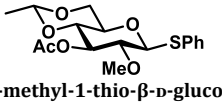

Phenyl 3-*O*-acetyl-4,6-*O*-ethylidene-2-*O*-methyl-1-thio-β-D-glucopyranose (S22). To a solution of **S21** (14 mg, 1 Eq, 45 µmol) pyridine (0.1 mL, 1 mmol) were added acetic anhydride (0.42 ml, 0.45 mmol, 10 equiv) and DMAP (0.55 mg, 4.5 µmol, 0.1 equiv). The reaction mixture was stirred at room temperature until TLC showed complete conversion after which it was concentrated *in vacuo.* The crude product was then dissolved in EtOAc and washed with sat. aq. $CuSO_4$. The organic layer was dried over $MgSO_4$, filtered and concentrated *in vacuo.* The crude material was then purified using silica gel flash column chromatography (100:0 → 70:30 *n*-heptane:EtOAc, v:v) to obtain phenyl 3-*O*-acetyl-2-*O*-methyl-4,6-*O*-ethylidene-1-thio-β-D-glucopyranose (10 mg, 0.028 mmol, 63 %) as a waxy solid. TLC: R_f 0.46 (EtOAc/*n*-heptane, 1:1 v/v); ^{1}H NMR (400 MHz, $CDCl_3$, HH-COSY, HSQC) δ 7.55 – 7.46 (m, 2H, CH_{arom}), 7.36 – 7.29 (m, 3H, CH_{arom}), 5.27 – 5.13 (m, 1H, H-3), 4.70 – 4.62 (m, 2H, H-1, CH_3CH), 4.21 – 4.13 (m, 1H, H-6), 3.53 (s, 4H, H-6, OCH_3), 3.40 – 3.30 (m, 2H, H-4, H-5), 3.19 (dd, *J* = 9.8, 8.8 Hz, 1H, H-2), 2.12 (s, 3H, CH_3 Ac), 1.31 (d, *J* = 5.1 Hz, 3H, CH_3CH). ^{13}C{^{1}H} NMR (101 MHz, $CDCl_3$) δ 170.0 ($C_{q\text{-}acetyl}$), 133.0, 132.5, 129.2, 128.1 (CH_{arom}), 99.7 (CH_3CH), 88.0 (C-1), 81.0 (C-2), 78.2 (C-4), 74.6 (C-3), 70.5 (C-5), 68.2 (C-6), 60.7 (OCH_3), 21.2 (CH_3 Ac), 20.4 (CH_3CH); HRMS (ESI): $[M + Na]^+$ Calcd for $C_{17}H_{22}O_6SNa$ 377.1035; found 377.1046.

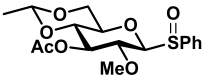

Phenyl 3-*O*-acetyl-4,6-*O*-ethylidene-2-*O*-methyl-1-thiosulfinyl-β-D-glucopyranose (5). A solution of **S22** (10 mg, 0.028 mmol) in DCM (1.0 ml, 0.05M) was cooled to –78 °C under inert atmosphere and then *meta*-chloroperoxybenzoic acid (1.1 equiv, 75 wt%) was added. The reaction was stirred for 3 h, diluted with DCM and washed with 10% aq. $Na_2S_2O_3$ solution, sat. aq. $NaHCO_3$ and brine. The organic layer was dried over $MgSO_4$, filtered, and concentrated *in vacuo*. The resulting crude mixture was used directly for IRMPD experiments. HRMS (ESI): $[M + Na]^+$ Calcd for $C_{17}H_{22}O_7SNa$, 393.0984; found, 393.0993.

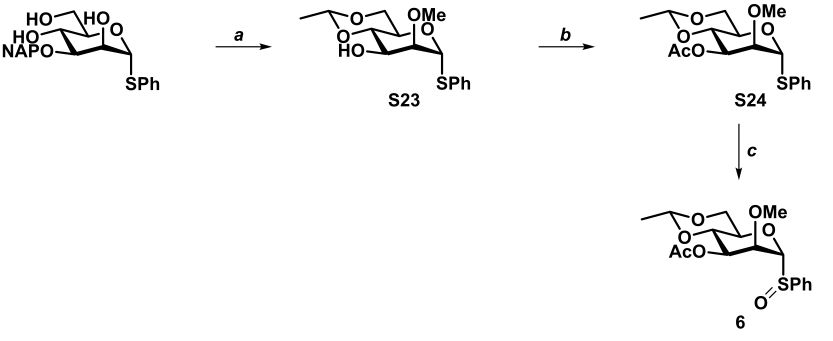

Supplementary scheme S4. Mannoside donor 6 synthesis. *Reagents and conditions:* a) 1. 1,1-dimethoxyethane, camphorsulfonic acid, acetonitril, RT; **2**. DDQ, DCM:H_2O, **S23**: 66%; b) acetic anhydride, pyridine, RT, **S24**: 63%; c) *meta*-chloroperoxybenzoic acid, DCM, **6**: quant.

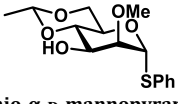

Phenyl 4,6-*O*-ethylidene-2-*O*-methyl-1-thio-α-D-mannopyranose (S23). To a solution of phenyl 2-*O*-methyl-3-*O*-(2-methyl)naphthyl-1-thio-α-D-mannopyranoside (250 mg, 0.59 mmol) in dry acetonitrile (5.9 ml, 0.1M) and 1,1-dimethoxyethane (1.76 mmol, 3 equiv), CSA (14 mg, 0.059 mmol, equiv) was added. The mixture stirred under argon atmosphere for 18 hours before being quenched by addition of triethylamine (0.10 mL). The resulting solution was concentrated *in vacuo*, diluted with EtOAc and washed with sat. aq. $NaHCO_3$ and brine. The organic layer was dried over $MgSO_4$, filtered and concentrated *in vacuo*. To a solution of the crude phenyl 2-*O*-methyl-3-*O*-(2-methyl)naphthyl-4,6-*O*-ethylidene-1-thio-α-D-glucopyranoside (200 mg, 0.44 mmol) in DCM/H_2O (7/1, 5 ml, 0.1M) was added DDQ (150 mg, 0.66 mmol, 1.5 equiv) and the reaction mixture was stirred in the dark to completion. The reaction mixture was diluted with DCM. The organic phase was washed twice using an aqueous mixture of ascorbic acid (0.7%), citric acid (1.5%) and NaOH (0.9%) (w/v). The organic layer way dried over $MgSO_4$, filtered and concentrated *in vacuo*. Flash column chromatography (100:0 → 70:30, *n*-heptane:EtOAc v:v) yielded the title compound (120 mg, 0.38 mmol, 87%) as a white waxy solid. TLC: R_f 0.21, (50:50, *n*-heptane:EtOAc, v:v); ^{1}H NMR (500 MHz, $CDCl_3$) δ 7.52 – 7.42 (m, 2H, CH_{arom}), 7.39 – 7.24 (m, 3H, CH_{arom}), 5.62 (d, *J* = 1.2 Hz, 1H, H-1), 4.77 (q, *J* = 5.0 Hz, 1H, CH_3CH), 4.15 (td, *J* = 9.8, 4.9 Hz, 1H, H-5), 4.03 (dd, *J* = 10.3, 4.9 Hz, 1H, H-6), 4.00 (d, *J* = 8.6 Hz, 1H, H-3), 3.82 (dd, *J* = 3.7, 1.3 Hz, 1H, H-2), 3.67 (t, *J* = 9.7 Hz, 1H, H-4), 3.60 (t, *J* = 10.3 Hz, 1H, H-6), 3.50 (s, 3H, OCH_3), 2.46 (bs, 1H, 3-O*H*), 1.39 (d, *J* = 5.1 Hz, 3H, CH_3CH); $^{13}C\{^1H\}$ NMR (126 MHz, $CDCl_3$) δ 133.8, 131.7, 129.3, 127.9 (CH_{arom}), 100.1 (*C*H ethylidene), 85.1 (C-1), 82.2 (C-2), 79.1 (C-4), 69.1 (C-3), 68.1 (C-6), 64.7 (C-5), 58.8 (OCH_3), 20.7 (CH_3CH); HRMS (ESI): $[M + Na]^+$ Calcd. for $C_{15}H_{20}O_5SNa$ 335.0929, found 335.0937.

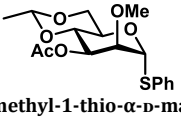

Phenyl 3-*O*-acetyl-4,6-*O*-ethylidene-2-*O*-methyl-1-thio-α-D-mannopyranose (S24). To a solution of **S23** (120 mg, 0.38 mmol) in pyridine (1.0 mL, 0.38M) were added acetic anhydride (0.5 ml, 0.45 mmol, 5 equiv) and DMAP (4.69 mg, 0.038 mmol, 0.1 equiv). The reaction mixture was stirred at room temperature for two hours after which it was concentrated *in vacuo.* The crude product was then dissolved in EtOAc and washed with sat. aq. $CuSO_4$ and brine. The organic layer was dried over $MgSO_4$, filtered and concentrated *in vacuo.* The crude material was then purified using silica gel flash column chromatography (100:0 → 80:20 *n*-heptane:EtOAc, v:v)

to obtain phenyl 3-*O*-acetyl-2-*O*-methyl-4,6-*O*-ethylidene-1-thio-β-D-mannopyranose (15 mg, 0.042 mmol, 11 %) as a waxy solid. TLC: R_f 0.42 (EtOAc/*n*-heptane, 1:1 v/v); ^{1}H NMR (500 MHz, $CDCl_3$) δ 7.52 – 7.42 (m, 2H, CH_{arom}), 7.40 – 7.16 (m, 3H, CH_{arom}), 5.56 (d, *J* = 1.4 Hz, 1H, H-1), 5.18 (dd, *J* = 10.5, 3.3 Hz, 1H, H-3), 4.75 (q, *J* = 5.0 Hz, 1H, CH_3CH), 4.25 (td, *J* = 9.9, 4.8 Hz, 1H, H-5), 4.04 (dd, *J* = 10.4, 4.9 Hz, 1H, H-6), 3.98 (dd, *J* = 3.4, 1.5 Hz, 1H, H-2), 3.93 (dd, *J* = 10.5, 9.4 Hz, 1H, H-4), 3.63 (t, *J* = 10.3 Hz, 1H, H-6), 3.44 (s, 3H, OCH_3), 2.15 (s, 3H, CH_3 Ac), 1.35 (d, *J* = 5.0 Hz, 3H, CH_3CH); ^{13}C{^{1}H} NMR (126 MHz, $CDCl_3$) δ 170.4 ($C_{q\text{-}acetyl}$), 133.9, 131.6, 129.3, 127.8 (CH_{arom}), 100.0 (CH_3CH), 85.8 (C-1), 80.2 (C-2), 75.8 (C-4), 70.9 (C-3), 68.1 (C-6), 65.2 (C-5), 59.2 (OCH_3), 21.2 (CH_3 Ac), 20.5 (CH_3CH).

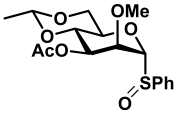

Phenyl 3-*O*-acetyl-4,6-*O*-ethylidene-2-*O*-methyl-1-thiosulfinyl-α-D-mannopyranose (6). A solution of **S23** (14.5 mg, 0.041 mmol) in DCM (1.0 ml, 0.05M) was cooled to –78 °C under inert atmosphere and then *meta*-chloroperoxybenzoic acid (1.1 equiv, 75 wt%) was added. The reaction was stirred for 3 h, diluted with DCM and washed with 10% aq. $Na_2S_2O_3$ solution, sat. aq. $NaHCO_3$ and brine. The organic layer was dried over $MgSO_4$, filtered, and concentrated *in vacuo*. The resulting crude mixture was used directly for IRMPD experiments. HRMS (ESI): $[M + Na]^+$ Calcd for $C_{17}H_{22}O_7SNa$, 393.0984; found, 393.0996.

References

(1) Nukada, T.; Berces, A.; Zgierski, M. Z.; Whitfield, D. M. Exploring the Mechanism of Neighboring Group Assisted Glycosylation Reactions. *J. Am. Chem. Soc.* **1998**, *120* (51), 13291–13295.

(2) Whitfield, D. M.; Nukada, T. DFT Studies of the Role of C-2–O-2 Bond Rotation in Neighboring-Group Glycosylation Reactions. *Carbohydr. Res.* **2007**, *342* (10), 1291–1304.

(3) Crich, D.; Dai, Z.; Gastaldi, S. On the Role of Neighboring Group Participation and Ortho Esters in β-Xylosylation: ^{13}C NMR Observation of a Bridging 2-Phenyl-1,3-Dioxalenium Ion. *J. Org. Chem.* **1999**, *64* (14), 5224–5229.

(4) Ishiwata, A.; Tanaka, K.; Ao, J.; Ding, F.; Ito, Y. Recent Advances in Stereoselective 1,2-*Cis*-*O*-Glycosylations. *Front. Chem.* **2022**, *10*, 972429.

(5) S. Nigudkar, S.; V. Demchenko, A. Stereocontrolled 1,2-*Cis* Glycosylation as the Driving Force of Progress in Synthetic Carbohydrate Chemistry. *Chem. Sci.* **2015**, *6* (5), 2687–2704.

(6) Das, R.; Mukhopadhyay, B. Chemical O-Glycosylations: An Overview. *ChemistryOpen* **2016**, *5* (5), 401–433.

(7) Andreana, P. R.; Crich, D. Guidelines for *O*-Glycoside Formation from First Principles. *ACS Cent. Sci.* **2021**, *7* (9), 1454–1462.

(8) Crich, D.; Sun, S. Are Glycosyl Triflates Intermediates in the Sulfoxide Glycosylation Method? A Chemical and ^{1}H, ^{13}C, and ^{19}F NMR Spectroscopic Investigation. *J. Am. Chem. Soc.* **1997**, *119* (46), 11217–11223.

(9) Crich, D.; Sun, S. Direct Chemical Synthesis of β-Mannopyranosides and Other Glycosides via Glycosyl Triflates. *Tetrahedron* **1998**, *54* (29), 8321–8348.

(10) Frihed, T. G.; Bols, M.; Pedersen, C. M. Mechanisms of Glycosylation Reactions Studied by Low-Temperature Nuclear Magnetic Resonance. *Chem. Rev.* **2015**, *115* (11), 4963–5013.

(11) Vorm, S. van der; Hansen, T.; S. Overkleeft, H.; Marel, G. A. van der; C. Codée, J. D. The Influence of Acceptor Nucleophilicity on the Glycosylation Reaction Mechanism. *Chem. Sci.* **2017**, *8* (3), 1867–1875.

(12) Komarova, B. S.; Orekhova, M. V.; Tsvetkov, Y. E.; Nifantiev, N. E. Is an Acyl Group at O-3 in Glucosyl Donors Able to Control α-Stereoselectivity of Glycosylation? The Role of Conformational Mobility and the Protecting Group at O-6. *Carbohydr. Res.* **2014**, *384*, 70–86.

(13) Crich, D.; Sharma, I. Influence of the O3 Protecting Group on Stereoselectivity in the Preparation of *C*-Mannopyranosides with 4,6-*O*-Benzylidene Protected Donors. *J. Org. Chem.* **2010**, *75* (24), 8383–8391.

(14) van der Vorm, S.; van Hengst, J. M. A.; Bakker, M.; Overkleeft, H. S.; van der Marel, G. A.; Codée, J. D. C. Mapping the Relationship between Glycosyl Acceptor Reactivity and Glycosylation Stereoselectivity. *Angew. Chem. Int. Ed.* **2018**, *57* (27), 8240–8244.

(15) Hengst, J. M. A. van; Hellemons, R. J. C.; Remmerswaal, W. A.; Vrande, K. N. A. van de; Hansen, T.; Vorm, S. van der; Overkleeft, H. S.; Marel, G. A. van der; Codée, J. D. C. Mapping the Effect of Configuration and Protecting Group Pattern on Glycosyl Acceptor Reactivity. *Chem. Sci.* **2023**, *14* (6), 1532–1542.

(16) Moumé-Pymbock, M.; Crich, D. Stereoselective C-Glycoside Formation with 2-*O*-Benzyl-4,6-*O*-Benzylidene Protected 3-Deoxy Gluco- and Mannopyranoside Donors: Comparison with *O*-Glycoside Formation. *J. Org. Chem.* **2012**, *77* (20), 8905–8912.

(17) Baek, J. Y.; Lee, B.-Y.; Jo, M. G.; Kim, K. S. β-Directing Effect of Electron-Withdrawing Groups at *O*-3, *O*-4, and *O*-6 Positions and α-Directing Effect by Remote Participation of 3-*O*-Acyl and 6-*O*-Acetyl Groups of Donors in Mannopyranosylations. *J. Am. Chem. Soc.* **2009**, *131* (48), 17705–17713.

(18) Ma, Y.; Lian, G.; Li, Y.; Yu, B. Identification of 3,6-Di-*O*-Acetyl-1,2,4-*O*-Orthoacetyl-α-D-Glucopyranose as a Direct Evidence for the 4-*O*-Acyl Group Participation in Glycosylation. *Chem. Commun.* **2011**, *47* (26), 7515–7517.
(19) Yao, D.; Liu, Y.; Yan, S.; Li, Y.; Hu, C.; Ding, N. Evidence of Robust Participation by an Equatorial 4-*O* Group in Glycosylation on a 2-Azido-2-Deoxy-Glucopyranosyl Donor. *Chem. Commun.* **2017**, *53* (20), 2986–2989.
(20) Crich, D.; Cai, W.; Dai, Z. Highly Diastereoselective α-Mannopyranosylation in the Absence of Participating Protecting Groups. *J. Org. Chem.* **2000**, *65* (5), 1291–1297.
(21) Crich, D.; Hu, T.; Cai, F. Does Neighboring Group Participation by Non-Vicinal Esters Play a Role in Glycosylation Reactions? Effective Probes for the Detection of Bridging Intermediates. *J. Org. Chem.* **2008**, *73* (22), 8942–8953.
(22) Hettikankanamalage, A. A.; Lassfolk, R.; Ekholm, F. S.; Leino, R.; Crich, D. Mechanisms of Stereodirecting Participation and Ester Migration from Near and Far in Glycosylation and Related Reactions. *Chem. Rev.* **2020**, *120* (15), 7104–7151.
(23) Crich, D. En Route to the Transformation of Glycoscience: A Chemist's Perspective on Internal and External Crossroads in Glycochemistry. *J. Am. Chem. Soc.* **2021**, *143* (1), 17–34.
(24) Remmerswaal, W. A.; Houthuijs, K. J.; van de Ven, R.; Elferink, H.; Hansen, T.; Berden, G.; Overkleeft, H. S.; van der Marel, G. A.; Rutjes, F. P. J. T.; Filippov, D. V.; Boltje, T. J.; Martens, J.; Oomens, J.; Codée, J. D. C. Stabilization of Glucosyl Dioxolenium Ions by "Dual Participation" of the 2,2-Dimethyl-2-(*Ortho*-Nitrophenyl)Acetyl (DMNPA) Protection Group for 1,2-*Cis*-Glucosylation. *J. Org. Chem.* **2022**, *87* (14), 9139–9147.
(25) Elferink, H.; Remmerswaal, W. A.; Houthuijs, K. J.; Jansen, O.; Hansen, T.; Rijs, A. M.; Berden, G.; Martens, J.; Oomens, J.; Codée, J. D. C.; Boltje, T. J. Competing C-4 and C-5-Acyl Stabilization of Uronic Acid Glycosyl Cations. *Chem. – Eur. J.* **2022**, *28*, e202201724.
(26) Hansen, T.; Elferink, H.; van Hengst, J. M. A.; Houthuijs, K. J.; Remmerswaal, W. A.; Kromm, A.; Berden, G.; van der Vorm, S.; Rijs, A. M.; Overkleeft, H. S.; Filippov, D. V.; Rutjes, F. P. J. T.; van der Marel, G. A.; Martens, J.; Oomens, J.; Codée, J. D. C.; Boltje, T. J. Characterization of Glycosyl Dioxolenium Ions and Their Role in Glycosylation Reactions. *Nat. Commun.* **2020**, *11* (1), 2664.
(27) Marianski, M.; Mucha, E.; Greis, K.; Moon, S.; Pardo, A.; Kirschbaum, C.; Thomas, D. A.; Meijer, G.; von Helden, G.; Gilmore, K.; Seeberger, P. H.; Pagel, K. Remote Participation during Glycosylation Reactions of Galactose Building Blocks: Direct Evidence from Cryogenic Vibrational Spectroscopy. *Angew. Chem. Int. Ed.* **2020**, *59* (15), 6166–6171.
(28) Greis, K.; Kirschbaum, C.; Fittolani, G.; Mucha, E.; Chang, R.; von Helden, G.; Meijer, G.; Delbianco, M.; Seeberger, P. H.; Pagel, K. Neighboring Group Participation of Benzoyl Protecting Groups in C3- and C6-Fluorinated Glucose. *Eur. J. Org. Chem.* **2022**, *2022* (15), e202200255.
(29) de Kleijne, F. F. J.; ter Braak, F.; Piperoudis, D.; Moons, P. H.; Moons, S. J.; Elferink, H.; White, P. B.; Boltje, T. J. Detection and Characterization of Rapidly Equilibrating Glycosylation Reaction Intermediates Using Exchange NMR. *J. Am. Chem. Soc.* **2023**, *145* (48), 26190–26201.
(30) Crich, D.; Li, W. Efficient Glycosidation of a Phenyl Thiosialoside Donor with Diphenyl Sulfoxide and Triflic Anhydride in Dichloromethane. *Org. Lett.* **2006**, *8* (5), 959–962.
(31) Codée, J. D. C.; Litjens, R. E. J. N.; den Heeten, R.; Overkleeft, H. S.; van Boom, J. H.; van der Marel, G. A. Ph_2SO/Tf_2O: A Powerful Promotor System in Chemoselective Glycosylations Using Thioglycosides. *Org. Lett.* **2003**, *5* (9), 1519–1522.
(32) Braak, F. ter; Elferink, H.; Houthuijs, K. J.; Oomens, J.; Martens, J.; Boltje, T. J. Characterization of Elusive Reaction Intermediates Using Infrared Ion Spectroscopy: Application to the Experimental Characterization of Glycosyl Cations. *Acc. Chem. Res.* **2022**, *55* (12), 1669–1679.
(33) Martens, J.; Berden, G.; Gebhardt, C. R.; Oomens, J. Infrared Ion Spectroscopy in a Modified Quadrupole Ion Trap Mass Spectrometer at the FELIX Free Electron Laser Laboratory. *Rev. Sci. Instrum.* **2016**, *87* (10), 103108.
(34) Oepts, D.; van der Meer, A. F. G.; van Amersfoort, P. W. The Free-Electron-Laser User Facility FELIX. *Infrared Phys. Technol.* **1995**, *36* (1), 297–308.
(35) Berden, G.; Derksen, M.; Houthuijs, K. J.; Martens, J.; Oomens, J. An Automatic Variable Laser Attenuator for IRMPD Spectroscopy and Analysis of Power-Dependence in Fragmentation Spectra. *Int. J. Mass Spectrom.* **2019**, *443*, 1–8.
(36) Hansen, T.; Lebedel, L.; Remmerswaal, W. A.; van der Vorm, S.; Wander, D. P. A.; Somers, M.; Overkleeft, H. S.; Filippov, D. V.; Désiré, J.; Mingot, A.; Bleriot, Y.; van der Marel, G. A.; Thibaudeau, S.; Codée, J. D. C. Defining the S_N1 Side of Glycosylation Reactions: Stereoselectivity of Glycopyranosyl Cations. *ACS Cent. Sci.* **2019**, *5* (5), 781–788.
(37) Demkiw, K. M.; Remmerswaal, W. A.; Hansen, T.; van der Marel, G. A.; Codée, J. D. C.; Woerpel, K. A. Halogen Atom Participation in Guiding the Stereochemical Outcomes of Acetal Substitution Reactions. *Angew. Chem. Int. Ed.* **2022**, *61*, e202209401.
(38) Chun, Y.; Remmerswaal, W. A.; Codée, J. D. C.; Woerpel, K. A. Neighboring-Group Participation by C-2 Acyloxy Groups: Influence of the Nucleophile and Acyl Group on the Stereochemical Outcome of Acetal Substitution Reactions. *Chem. – Eur. J.* **2023**, *29*, e202301894.

(39) Hosoya, T.; Kosma, P.; Rosenau, T. Theoretical Study on the Effects of a 4,6-O-Diacetal Protecting Group on the Stability of Ion Pairs from D-Mannopyranosyl and D-Glucopyranosyl Triflates. *Carbohydr. Res.* **2015**, *411*, 64–69.
(40) de Kleijne, F. F. J.; Elferink, H.; Moons, S. J.; White, P. B.; Boltje, T. J. Characterization of Mannosyl Dioxanium Ions in Solution Using Chemical Exchange Saturation Transfer NMR Spectroscopy. *Angew. Chem. Int. Ed.* **2022**, *61* (6), e202109874.
(41) van Outersterp, R.E.; Houthuijs, K.J.; Berden, G.; Engelke, U.F.; Kluijtmans, L.A.J.; Wevers, R.A.; Coene, K.L.M.; Oomens, J.; Martens, J.; Molecular Spectroscopy (HIMS, FNWI). Reference-Standard Free Metabolite Identification Using Infrared Ion Spectroscopy. *Int. J. Mass Spectrom.* **2019**, *443*, 77–85.
(42) To corroborate the effect of the C-2 substituent, the reaction profile of the C-2-deoxy system was generated in a similar manner. The potential energy surface for the formation of the 1,3-dioxanium ion from the 2-deoxy-3-*O*-benzoyl-4,6-*O*-ethylidene glucosyl triflate was indeed shown to be very similar, in terms of both structure and energy, to that of its mannosyl counterpart (Supplementary figure S4).
(43) Santana, A. G.; Montalvillo-Jiménez, L.; Díaz-Casado, L.; Corzana, F.; Merino, P.; Cañada, F. J.; Jiménez-Osés, G.; Jiménez-Barbero, J.; Gómez, A. M.; Asensio, J. L. Dissecting the Essential Role of Anomeric β-Triflates in Glycosylation Reactions. *J. Am. Chem. Soc.* **2020**, *142* (28), 12501–12514.
(44) Additional reaction profiles of the 2,4,6-tri-*O*-methyl-3-*O*-benzoyl-glycosyl and 2-*O*-methyl-3-*O*-(4-*O*-methyl-benzoyl)-4,6-*O*-ethylidene-glycosyl donors can be found in Supplementary Figure S5, S6 and Table S1.
(45) Huang, M.; Retailleau, P.; Bohé, L.; Crich, D. Cation Clock Permits Distinction Between the Mechanisms of α- and β-*O*- and β-*C*-Glycosylation in the Mannopyranose Series: Evidence for the Existence of a Mannopyranosyl Oxocarbenium Ion. *J. Am. Chem. Soc.* **2012**, *134* (36), 14746–14749.
(46) Huang, M.; Garrett, G. E.; Birlirakis, N.; Bohé, L.; Pratt, D. A.; Crich, D. Dissecting the Mechanisms of a Class of Chemical Glycosylation Using Primary ^{13}C Kinetic Isotope Effects. *Nat. Chem.* **2012**, *4* (8), 663–667.
(47) Legault, C. Y. CYLview, 1.0b, Université de Sherbrooke, 2009. http://www.cylview.org.
(48) Landrum, G.; Tosco, P.; Kelley, B.; Ric; Sriniker; Gedeck; Vianello, R.; NadineSchneider; Kawashima, E.; Dalke, A.; N, D.; Cole, B.; Cosgrove, D.; Swain, M.; Turk, S.; AlexanderSavelyev; Jones, G.; Vaucher, A.; Wójcikowski, M.; Probst, D.; Scalfani, V. F.; Godin, G.; Pahl, A.; Berenger, F.; JLVarjo; Ujihara, K.; Strets123; JP; DoliathGavid; Sforna, G. RDKit, 2022.
(49) Frisch, M. J.; Trucks, G. W.; Schlegel, H. B.; Scuseria, G. E.; Robb, M. A.; Cheeseman, J. R.; Scalmani, G.; Barone, V.; Petersson, G. A.; Nakatsuji, H.; Li, X.; Caricato, M.; Marenich, A. V.; Bloino, J.; Janesko, B. G.; Gomperts, R.; Mennucci, B.; Hratchian, H. P.; Ortiz, J. V.; Izmaylov, A. F.; Sonnenberg, J. L.; Williams; Ding, F.; Lipparini, F.; Egidi, F.; Goings, J.; Peng, B.; Petrone, A.; Henderson, T.; Ranasinghe, D.; Zakrzewski, V. G.; Gao, J.; Rega, N.; Zheng, G.; Liang, W.; Hada, M.; Ehara, M.; Toyota, K.; Fukuda, R.; Hasegawa, J.; Ishida, M.; Nakajima, T.; Honda, Y.; Kitao, O.; Nakai, H.; Vreven, T.; Throssell, K.; Montgomery Jr., J. A.; Peralta, J. E.; Ogliaro, F.; Bearpark, M. J.; Heyd, J. J.; Brothers, E. N.; Kudin, K. N.; Staroverov, V. N.; Keith, T. A.; Kobayashi, R.; Normand, J.; Raghavachari, K.; Rendell, A. P.; Burant, J. C.; Iyengar, S. S.; Tomasi, J.; Cossi, M.; Millam, J. M.; Klene, M.; Adamo, C.; Cammi, R.; Ochterski, J. W.; Martin, R. L.; Morokuma, K.; Farkas, O.; Foresman, J. B.; Fox, D. J. Gaussian 16 Rev. C.01, 2016.
(50) Frisch, M. J.; Trucks, G. W.; Cheeseman, J. R.; Scalmani, G.; Caricato, M.; Hratchian, H. P.; Li, X.; Barone, V.; Bloino, J.; Zheng, G.; Vreven, T.; Montgomery, J. A.; Petersson, G. A.; Scuseria, G. E.; Schlegel, H. B.; Nakatsuji, H.; Izmaylov, A. F.; Martin, R. L.; Sonnenberg, J. L.; Peralta, J. E.; Heyd, J. J.; Brothers, E.; Ogliaro, F.; Bearpark, M.; Robb, M. A.; Mennucci, B.; Kudin, K. N.; Staroverov, V. N.; Kobayashi, R.; Normand, J.; Rendell, A.; Gomperts, R.; Zakrzewski, V. G.; Hada, M.; Ehara, M.; Toyota, K.; Fukuda, R.; Hasegawa, J.; Ishida, M.; Nakajima, T.; Honda, Y.; Kitao, O.; Nakai, H. Gaussian 09 Rev. D.01, 2009.
(51) Spartan'14, Wavefunction, Inc., Irvine, CA.
(52) Halgren, T. A. Merck Molecular Force Field. I. Basis, Form, Scope, Parameterization, and Performance of MMFF94. *J. Comput. Chem.* **1996**, *17* (5–6), 490–519.
(53) Hansen, T.; Lebedel, L.; Remmerswaal, W. A.; van der Vorm, S.; Wander, D. P. A.; Somers, M.; Overkleeft, H. S.; Filippov, D. V.; Désiré, J.; Mingot, A.; Bleriot, Y.; van der Marel, G. A.; Thibaudeau, S.; Codée, J. D. C. Defining the SN1 Side of Glycosylation Reactions: Stereoselectivity of Glycopyranosyl Cations. *ACS Cent. Sci.* **2019**, *5* (5), 781–788.
(54) Ribeiro, R. F.; Marenich, A. V.; Cramer, C. J.; Truhlar, D. G. Use of Solution-Phase Vibrational Frequencies in Continuum Models for the Free Energy of Solvation. *J. Phys. Chem. B* **2011**, *115* (49), 14556–14562.
(55) Luchini, G.; Alegre-Requena, J. V.; Funes-Ardoiz, I.; Paton, R. S. GoodVibes: Automated Thermochemistry for Heterogeneous Computational Chemistry Data. *F1000Research* **2020**, *9*, 291.
(56) OriginPro, 9.0.0. OriginLab Corporation, Northampton, MA, USA.